**HRS-WASH axis governs Actin mediated endosomal recycling and cell invasion.**

Ewan MacDonald[1,3], Louise Brown[1], Arnaud Selvais[1], Han Liu[2], Thomas Waring[1], Daniel Newman[1], Jessica Bithell[1], Douglas Grimes[1], Sylvie Urbé[1], Michael J. Clague[1] and Tobias Zech[1].

[1] Institute of Translational Medicine, Cellular and Molecular Physiology, University of Liverpool, UK.

[2] Institute of Cancer Stem Cell, Dalian Medical University, Dalian 116044, China

[3] present address: Institut Curie, PSL Research University, Cellular and Chemical Biology unit, INSERM U 1143, CNRS UMR 3666, 26 rue d'Ulm, 75248 Paris Cedex 05, France.

**Abstract**

Transmembrane proteins in the sorting endosome are either recycled to their point of origin or destined for lysosomal degradation. Lysosomal sorting is mediated by interaction of ubiquitylated transmembrane proteins with the ESCRT-machinery. Here, we uncover an alternative role for the ESCRT-0 component HRS in promoting the constitutive recycling of transmembrane proteins. We find that endosomal localisation of the Actin nucleating factor WASH requires HRS, which occupies adjacent endosomal sub-domains. Depletion of HRS results in defective constitutive recycling of EGFR and the metalloproteinase MT1-MMP leading to their accumulation in internal compartments. We show that direct interactions with endosomal Actin are required for efficient recycling and use a model system of chimeric Transferrin receptor trafficking to show that an Actin-binding motif can counteract an ubiquitin signal for lysosomal sorting. Directed receptor recycling is utilised by cancer cells to achieve invasive migration. Accordingly, abrogating HRS and Actin dependent MT1-MMP recycling results in defective matrix degradation and invasion of triple negative breast cancer cells.

**eTOC Summary**

ESCRT-0 component HRS and Actin polymerization factor WASH reside in adjacent endosomal domains. MacDonald et al. show that HRS controls WASH localization and recycling of WASH dependent transmembrane cargo. Cargo binding to endosomal actin thus acts as sorting signal to oppose ubiquitin-mediated degradation.

**Introduction**

Cell surface proteins that enter endosomes may be recycled to the plasma membrane or otherwise actively sorted towards the lysosomal pathway. The latter pathway has been well characterised in the case of ubiquitylated receptors, which engage with components of the ESCRT (Endosomal Sorting Complexes Required for Transport) machinery (Henne et al., 2011; Williams

and Urbe, 2007). The ESCRT-0 complex, comprising HRS and STAM, provides multiple ubiquitin interaction surfaces as well as recruiting the ESCRT-I complex via interactions between HRS and TSG101 (Bache et al., 2003; Clague and Urbe, 2003; Pornillos et al., 2003). HRS is recruited to endosomes via its FYVE domain, which interacts with locally generated PtdIns3*P* (Urbe et al., 2000). The sorting endosome is sub-compartmentalised into tubular and vacuolar aspects and shows segregation of proteins to specific domains within the same limiting membrane (Luini et al., 2005).

Ubiquitin is an established signal for sorting into the multivesicular body (MVB), a structure that forms upon endosome maturation. Several motifs have also been established to promote receptor endocytosis (Lauwers et al., 2009). However, no unifying intrinsic sequence has been found that affects recycling from endosomes (Apodaca et al., 1994; Gruenberg, 2001; Jing et al., 1990). The pathway must accommodate bountiful and highly dynamic shuttling receptors for internalised intracellular nutrients, such as the Transferrin receptor, as well as provide an escape route for receptors and other plasma membrane components that have not been marked for degradation. The prevailing early view was that it largely represents a bulk-flow process (Mayor et al., 1993). Recent work has suggested that the WASH (Wiscott-Aldrich syndrome protein and SCAR homologue) complex in association with defined retromer complexes mediates the recycling of specific plasma membrane proteins (Steinberg et al., 2013). A more complex feature of the recycling pathway is represented by its ability to distribute to different regions of the cell, for example the leading edge of migrating cells or one or other membrane of polarised cells (Matter and Mellmann, 1994). Such recycling of MT1-MMP and EGFR drives cancer cell invasion (Caswell et al., 2008; Steffen et al., 2008).

The WASH complex is an endosomal Arp2/3 activator that stimulates the polymerisation of filamentous Actin (F-Actin) (Derivery et al., 2009; Gomez and Billadeau, 2009). It facilitates retrograde trafficking from endosomes to Golgi (ci-M6PR (Gomez and Billadeau, 2009)) and recycling from endosomes to the plasma membrane (α5β1 integrin (Zech et al., 2011), LDL receptor (Bartuzi et al., 2016)). Currently, the mechanisms of WASH complex recruitment and activation are only partially understood. An interaction between FAM21 and the retromer component VPS35 was shown to be important for the recruitment of the WASH complex onto endosomes and phospholipid binding may play a role in its membrane targeting (Harbour et al., 2012; Helfer et al., 2013) (Jia et al., 2010). Interestingly, WASH activity can be controlled through reversible ubiquitylation, which stabilises the WASH complex in its active form (Hao et al., 2013; Hao et al., 2015). Depletion of WASH has been reported to result in elongated tubules emanating from the endosome and as such WASH is thought to participate in membrane fission through an interaction with dynamin (Derivery et al., 2009). F-Actin is required for the stabilisation of tubules that are utilised for sorting of receptors and it has been proposed that direct and indirect interactions between transmembrane proteins and Actin sequesters receptors for recycling (Carnell et al., 2011; Puthenveedu et al., 2010; Zech et al., 2012). In the present study we took

advantage of two known Actin binding domains in the EGFR receptor (den Hartigh et al., 1992) and the metalloproteinase MT1-MMP (Yu et al., 2012) to investigate their influence on retrograde trafficking. We provide evidence that WASH mediated receptor recycling and ESCRT driven degradation at the endosome are functionally coupled by virtue of a shared requirement for the ESCRT-0 component HRS. WASH localisation to the endosome is dependent on HRS while the two systems compete for the sorting of receptors into respective subdomains. We identify the function of the intrinsic Actin binding domains of EGFR and MT1-MMP as directing the default sorting to recycling under steady state conditions and show that HRS orchestrated endosomal Actin is required for MT1-MMP dependent invasive cell migration of breast cancer cells.

## Results

*HRS occupies a separate sub-domain but is required for the recruitment of WASH to endosomes*

Co-staining of fixed cells with WASH and HRS antibodies revealed a high degree of co-localization in HeLa and MDA-MB-231 cells (Figs. 1A; S1A). We further utilised a HeLa Flp-In$^{TM}$cell line stably expressing GFP-tagged mouse HRS (GFP-mHRS) at near endogenous levels, to transiently express mCherry-mWASH. Again we observed a high degree of overlap between the two proteins and their co-migration on dynamic endosomes (Vid.1). Nevertheless, using Airyscan based super-resolution microscopy to image at 100nm resolution, we could resolve spatial differences representing their concentration in adjacent subdomains of the endosome (Fig.1B). In order to confirm this, we used overexpression of a constitutively active form of Rab5 (Rab5Q79L), which induces the formation of large endosomes by promoting homotypic fusion (Barbieri et al., 1996). Co-staining these cells for WASH and HRS, we observed a separation of WASH and HRS domains on the limiting membrane (Fig. S1B). In order to investigate how closely juxtaposed these endosomal subdomains are, we used a proximity ligation assay that showed that HRS and WASH can be found within 40nm distance from each other, the maximum working distance of this assay (Fig. 1C&D; S1C). These orthogonal experiments demonstrate that WASH and HRS are localised to the same endosome in HeLa cells but are separated out into adjacent sub-domains on the limiting membrane.

We next sought to determine if there was a functional relationship between HRS and WASH. We depleted either HRS or WASH using siRNA. Whilst WASH depletion did not interfere with HRS localisation, depletion of HRS resulted in the loss of WASH staining at endosomes in both HeLa and MDA-MB-231 cells (Fig. 1A,F,G; S1A,D,E). Using EEA1 as an endosomal marker in HRS depleted cells, we saw a concomitant loss of endosomal F-Actin and Arp2/3 complex that is a predicted consequence of the mis-localisation of WASH (Fig.1H&I; S1F&G).

Immunoblot analysis of HRS depleted HeLa cells revealed that there was a similar reduction in WASH (% of siNT, siHRS-1=71+/-16%, siHRS-2=58+/-3%) and the retromer component VPS35 (% of siNT, siHRS-1=60+/-6%, siHRS-2=46+/-3%) protein levels in HeLa cells,

but in MDA-MB-231 cells we observed no significant changes in the levels of WASH, despite the observed loss of WASH staining from the endosome (Fig. S2A-F). To confirm that the loss of WASH from endosomes was caused by the depletion of HRS, we performed parallel experiments in isogenic Flp-In$^{TM}$ cell lines expressing either GFP or GFP-mHRS (Fig. 1E). In control GFP expressing cells, the early endosomal marker EEA1 and WASH co-localised (R= (Pearson's R coefficient) = 0.33 +/- 0.02) but following endogenous HRS depletion with siRNA targeting human HRS this was reduced to background levels (R=0.08+/-0.055). However, in the cell lines expressing siRNA resistant GFP-mHRS there were no measurable differences in the co-localisation of WASH with EEA1 (GFP-mHRS + siHRS R= 0.34 +/-0.1) following treatment with the same siRNA oligonucleotides (Fig. 1F&G). We observed no loss in the endosomal pool of VPS35 or the COMMD/CCDC22/CCDC93 (CCC) complex member COMMD1 that is also linked to the WASH complex (Fig.2A-C; S1H&I) (Phillips-Krawczak et al., 2015). This confirms that HRS expression is specifically required for correct localisation and function of WASH.

In order to test if the dynamics of WASH recruitment onto the endosomal membrane are governed by HRS, we performed fluorescence recovery after photo-bleaching (FRAP) experiments using mCherry-WASH (Fig.2D). HeLa cells were depleted of HRS using siRNA and then transfected with GFP-EEA1 and mCherry-WASH. WASH and EEA1 positive endosomes were subjected to photobleaching and the recovery of mCherry-WASH was measured. There was a significant decrease in the rate of recovery following HRS depletion (siNT k=0.504 +/- 0.071, siHRS k=0.171 +/- 0.046 (k=secs$^{-1}$) TTest p=<0.01) (Fig. 2E). In contrast, there was no observable change in the recruitment dynamics of VPS35 after HRS depletion (Fig. 2F&G). Taken together, the data demonstrate that HRS is required for the correct recruitment and localisation of WASH to endosomes.

We sought to identify domains in HRS responsible for the recruitment of WASH to endosomes. We tested several HRS domain deletion constructs, known to retain endosomal localisation, and found that expression of the combined VHS-FYVE domain alone was sufficient to rescue the endosomal localisation of WASH (Fig. S3A-C). The FYVE domain is necessary for the recruitment of HRS onto endosomes in a PtdIns3*P* dependent manner (Urbe et al., 2000), whilst the VHS domain is thought to act as an interaction module. In GGA proteins, the VHS domain can directly bind to cargo in order to facilitate retrograde transport (Mao et al., 2000; Puertollano et al., 2001). We tested whether HRS mediated WASH recruitment is sensitive to cargo accumulation at the endosome. We used 100µM Primaquine to block recycling of transmembrane proteins in HeLa cells and observed that this led to accumulation of GFP-VHS-FYVE, EGFR and WASH, but not the PtdIns3*P* sensor GFP-FENS-FYVE, on the endosomal membrane (Fig. S3D-F and data not shown).

*HRS is required for the Actin mediated recycling of WASH dependent cargo*

The preceding results suggested that HRS may be able to govern endosomal recycling of specific receptors through recruitment of WASH and localised control of actin dynamics. To check

this, we initially monitored the distribution of cation independent mannose-6-phosphate receptor (ci-M6PR), a transmembrane protein that shuttles between the Trans-Golgi network (TGN) and endosomes. At steady state in control HeLa cells, ci-M6PR was localized to the TGN. After depletion of HRS or WASH, ci-M6PR redistributed to EEA1 positive endosomes away from TGN46 (Figs. S4A-D). In the absence of ci-M6PR recycling from the endosome back to the TGN, the receptor cannot engage with any newly synthesised acid hydrolases, such as Cathepsin D, which are therefore mis-sorted at the TGN and secreted into the extracellular environment (Lobel et al., 1989). We precipitated proteins from conditioned media of either control or HRS depleted HeLa cells. In HRS depleted cells we observed an increase in the levels of immature Cathepsin D in the medium providing biochemical evidence for a defect in ci-M6PR shuttling (Fig. S4E).

We next tested if HRS depletion had an effect on the steady state trafficking of endogenous EGFR, which is also known to accumulate in endosomes after loss of WASH (Gomez et al., 2012). Under steady state conditions there was an accumulation of EGFR in an EEA1 positive endosomal compartment but not the trans Golgi network in HeLa (Fig. 3A&B; S4F) and MDA-MB-231 cells (Fig. 3C&D). We observed a concomitant loss of cell surface EGFR levels (Fig. 3E), but no significant change in total EGFR levels after HRS depletion (Fig. 3F). To ascertain that the accumulation of EGFR was due to defective retrograde traffic under our experimental conditions, we blocked endosomal receptor recycling with Primaquine and observed a comparable accumulation of EGFR in endosomes (Fig. S3F). We used photoactivatable GFP coupled to EGFR (EGFR-paEGFP) to determine whether this EGFR accumulation was caused by a failure to recycle EGFR out of endosomes and to directly measure the residence time of the receptor in Rab4 positive endosomes in HeLa cells. After HRS depletion there was a significant decrease in the rate of EGFR exit from the endosome compared to control cells (siNT k=0.0462+/-0.0168, siHRS k=0.0215+/-0.011, ($k=sec^{-1}$), TTest p=<0.01) (Fig. 3G, Vid.2). To further confirm this observation, we performed biochemical EGFR trafficking ELISA assays based on reversible biotinylation that showed a significant reduction in the percentage of receptor that was recycled (Fig. 3H, TTest p=<0.01).

To determine if HRS had an effect on trafficking of activated EGFR we serum staved HeLa cells for two hours before stimulation with 1ng/ml EGF, an experimental setup that has previously been identified to increase the internalisation rate of the receptor, but not the degradation of the receptor (Sigismund et al., 2013). We did not see significant changes in the degradation rate of EGFR in HeLa cells treated with 1ng/ml EGF upon loss of HRS compared to wild type cells (Fig. 4A&B). We did however observe an increase in the levels of EGFR in EEA1 positive endosomes in HRS depleted cells after 30mins compared to control cells (Fig. 4C-G). As there was no change in the EGFR protein levels, we conclude that the change in distribution of EGFR upon HRS loss is due to changes in the ability of the EGFR to recycle out of the EEA1/VPS35/WASH positive endosomes.

To confirm our results with another WASH complex dependent cargo, we next looked at trafficking of the pro-invasive matrix metalloproteinase MT1-MMP in the triple negative breast cancer cell line MDA-MB-231 (Monteiro et al., 2013). HRS depleted and control MDA-MB-231 cells

were stained for endogenous MT1-MMP, this showed a concentration of MT1-MMP in retromer positive endosomal compartments that was greatly increased upon HRS depletion (Figs. 5A&B, S5A). The dynamics of MT1-MMP recycling from endosomes were tested by transfection with a photoactivatable mCherry-MT1-MMP (paCherry-MT1-MMP) construct and GFP-EEA1. We observed that there was a significant delay in the recycling of the receptor from the endosome (Fig.5C). These results confirm a robust blockade in the recycling of WASH dependent cargo upon HRS depletion.

*Direct Actin binding of receptors is required for efficient endosomal sorting*

As loss of the HRS/WASH axis caused a decrease in endosomal F-Actin and a blockade in recycling. Thus we wondered if proteins could directly or indirectly bind to F-Actin to facilitate this transport step (Zech et al., 2012). To test this hypothesis, we used two recycling proteins that have previously been demonstrated to directly bind to Actin, the EGFR (den Hartigh et al., 1992) and MT1-MMP (Yu et al., 2012). We mutated the previously identified minimal sequences required for Actin binding for both EGFR and MT1-MMP, YLIP/AAAA (1016-1019) and LLY/AAA (571-573) respectively, in order to assess changes in the localisation and trafficking of the receptors. To investigate Actin dependent EGFR recycling, we employed photo-activation experiments from mCherry-Rab4 positive endosomes. We observed quicker sorting of the wild type receptor into vesicles emanating from Rab4 positive endosomes (Fig. 6A&B; Vid. 3), whilst the Actin binding deficient receptors were excluded from the bulk of tubules (Fig. 6A&B; Vid. 3). We could also observe gross changes in the localisation of our overexpressed constructs, with the YLIP/AAAA being predominantly confined to endosomes while the wild type EGFR showed more cell surface expression (Vid.4). By using primaquine as a positive control for recycling inhibition (van Weert et al., 2000), we could establish that blockade of receptor recycling causes a corresponding stabilisation of the fluorescence signal in the endosome (Fig. 6B; Vid. 5). There was a significant decrease in the rate of exit of the Actin binding deficient EGFR from the endosomes compared to the wild type receptor (WT k=0.0493 +/- 0.0038, AAAA k=0.0297 +/- 0.0028, TTest p=0.02, n=4 individual experiments ($k=sec^{-1}$)). When we tested the trafficking dynamics of photoactivated paCherry-MT1-MMP constructs out of EEA1-GFP positive endosomes, we observed an almost complete blockade in the trafficking of the ABD mutant MT1-MMP LLY/AAA constructs (Fig. 6C, Vid.6). These results show that the recycling of EGFR and MT1-MMP out of the endosome is dependent upon the ability of the receptors to directly interact with Actin.

*Direct Actin binding can overcome ubiquitin mediated sorting at the endosome*

Our findings showing that HRS governs receptor recycling contrasts with a body of previous work linking it to the active sorting of ubiquitylated receptors into the lumen of multivesicular bodies. Sorting towards degradation or recycling is a crucial decision in receptor

transport. We wanted to examine if there is competition between Actin binding required for retrograde transport and ubiquitin mediated sorting into multivesicular bodies. In order to achieve this, we employed a previously described assay (Raiborg et al., 2002) where a non-cleavable moiety of Ubiquitin is fused to the intracellular tail of Transferrin receptor (TrfR). Normally TrfR is efficiently recycled, however the fusion of a single ubiquitin moiety is sufficient to sort the receptor via HRS and receptor sorting towards degradation. We added the Actin binding region of the cytoplasmic tail of MT1-MMP to the TrfR adjacent to a non-cleavable Ubiquitin moiety (Ub-ABD-TrfR), creating a direct competition for the sorting of the chimeric receptor between ubiquitin and actin mediated sorting (Fig. 7A).

HeLa cells were transfected with the wild type TrfR, Ub-TrfR conjugate or Ub-ABD-TrfR (Fig. S5B). Transfected cells were incubated for 15mins with FITC coupled Transferrin (Trf) to achieve equilibrium loading (Fig. 7B). Fresh media with unlabelled Transferrin was added to the cells and the receptor ligand complexes were allowed to recycle for an hour. The Ub-TrfR construct was retained in endosomes and the construct showed a higher degree of co-localisation with FITC-Trf after one hour chase compared to the WT or Ub-ABD-TrfR (Fig. 7C). This mirrored results previously reported with the Ub-TrfR construct, whereas the WT and Ub-ABD-TrfR recycled back to the plasma membrane and released the FITC-Trf as observed by a significantly reduced association with FITC-TrfR (Fig. 7B&C) (TrfR R=0.29, Ub-TrfR R=0.4346, Ub-ABD-TrfR R=0.3013).

To characterise the dynamics of this sorting event we employed a flow cytometry assay. HeLa S3 cells were transfected and loaded with FITC-Trf for 15mins before removal and fixation at the indicated time points and analysis by flow cytometry. After 30mins there was a 30.8% (+/-6.3%) increase in retention of the Ub-TrfR compared to wild type receptor whereas the Actin binding domain containing Ub-ABD-TrfR construct had identical recycling dynamics as the WT receptor (Fig. 7D). We next tested whether the chimeric receptors had been redirected into the degradative pathway by the addition of the non-cleavable ubiquitin. In order to do this, we performed cycloheximide chases blocking protein synthesis. The Ub-TrfR had a significantly increased rate of degradation compared to the wild type receptor over an eight-hour time course indicating that the receptor is being sorted towards lysosomal degradation. In contrast, the addition of the actin-binding domain was able to rescue the effect of coupling ubiquitin to the TrfR with the chimeric receptor having identical degradation rates as the wild type receptor (Fig. 7E&F). Our data demonstrate that Actin binding can overcome mono-ubiquitin mediated endosomal sorting.

*WASH/HRS axis is required for cell invasion*

MT1-MMP is a pivotal matrix metalloproteinase required for degradation of matrix proteins to enable cancer cell invasion into non-permissive extracellular matrix (Hotary et al., 2006; Hotary et al., 2003; Sabeh et al., 2004). We sought to test if HRS dependent recycling has a functional

role in cancer cell properties that could be ascribed to MT1-MMP dynamics. We analysed whether the HRS/WASH axis was required for MT1-MMP dependent triple negative breast cancer cell matrix degradation, migration, and invasion. To assess invadopodia based degradation ability, MDA-MB-231 cells were depleted of HRS using siRNA and seeded onto coverslips coated with labelled gelatin overnight. There was a significant decrease in the ability of HRS depleted cells to degrade gelatin over 16 hours (Fig. 8A&B). We observed no change in the ability of MDA-MB-231 cells to migrate over plastic indicating that the cells maintained the essential migration machinery (Fig. S5C-F). An inverted invasion assay, into a gel composed of Matrigel and fibronectin, showed a significant decrease in invasion capacity of HRS and WASH depleted cells, which was indistinguishable from cells treated with the metalloproteinase inhibitor GM6001 or MT1-MMP knockdown (Fig. 8C&D). Cross-linked Collagen I provides a more realistic substrate barrier for cancer cell invasion, with the pore size inhibiting any migration unless there is accompanying matrix degradation (Wolf et al., 2009; Wolf and Friedl, 2009). MDA-MB-231 cells were depleted of HRS or WASH and seeded onto fibroblast remodeled organotypic collagen gels for 2-3 days, before culture at the liquid-air interphase for 7 days. The silencing or HRS and WASH significantly reduced invasion by 40-50% (Fig. 8E&F). These experiments support the model that the HRS/WASH axis is important for breast cancer cell invasion.

**Discussion**

HRS is constitutively associated with STAM to form the core of the ESCRT-0 complex. A body of data exists linking this complex to the capture of ubiquitylated proteins and to recruitment of the ESCRT-I complex. It is a key element of the ESCRT machinery devoted to directing proteins into MVBs for transport to lysosomes. Other aspects of HRS function have also been reported. It has been described to dictate the retrograde trafficking of the β-adreno and TrKB receptors through an unknown mechanism, that depends on the expression of the VHS and FYVE domains of HRS (Hanyaloglu and von Zastrow, 2007; Huang et al., 2009). Here, we uncover a key role for HRS in the endosomal association and activity of the Actin polymerisation factor WASH. We show that this axis governs the recycling to the plasma membrane of proteins that contain defined Actin binding motifs (EGFR, MT1-MMP).

WASH complex localisation had previously been defined to span Rab4, EEA1 and Rab7 positive endosomes, that are considered to be receptor recycling competent (Dozynkiewicz et al., 2012; Macpherson et al., 2014; Zech et al., 2011). Previous studies have shown a role for the retromer component VPS35 in the recruitment of WASH to endosomes (Harbour et al., 2010; Harbour et al., 2012; Jia et al., 2012). Direct interactions of VPS35 and the retromer associated Sorting Nexins 1&3 (Snx1&3) with HRS have been reported, that could potentially provide a link to the WASH complex (Pons et al., 2008; Popoff et al., 2009). Despite a decrease in the total pool of VPS35 in HRS depleted HeLa cells, we saw no changes in the endosomal pool of VPS35 in HeLa and MDA-MB-231 cells. This is in agreement with studies showing at least partial retromer independent endosomal WASH recruitment in Dictyostelium (Park et al., 2013) and mouse VPS35

knock-out cells (McNally et al., 2017). A recent study has identified a retromer analogous complex called Retriever that is required for retrograde trafficking of WASH dependent cargo, for example α5β1 integrin, through a WASH-FAM21-CCC complex-Retriever cascade (Bartuzi et al., 2016; McNally et al., 2017). We did not observe a reduction in endosomal levels of the CCC complex member COMMD1 after HRS depletion, but it will interesting to see whether HRS and the interplay with the degradation pathway will have an impact on endosomal Retriever dynamics and activity.

Rather than being a retromer only dependent recruitment process for WASH on the endosome, we found that a minimal construct of HRS encompassing a FYVE domain and adjacent VHS domain (VHS-FYVE) is sufficient for WASH recruitment to endosomes. The FYVE domain of HRS is necessary for its recruitment to endosomes through binding to the inositol lipid PtdIns3*P*, whose levels we find to be unchanged following HRS depletion (Raiborg et al., 2001; Urbe et al., 2000). The VHS domain has a less clear function. It forms a "superhelix" of eight alpha helices that can behave as a multipurpose docking site capable of binding to membranes and proteins (Mao et al., 2000). The VHS domains in GGA proteins have been shown to directly interact with cargo (Misra et al., 2002; Puertollano et al., 2001), while the VHS-FYVE domain of HRS can directly bind to ubiquitin chains (Ren and Hurley, 2010). Whilst we have no evidence for direct HRS-WASH complex binding, we speculate that this minimal component can either recruit an adaptor protein or otherwise configure endosomal domain architecture to enable binding.

We confirmed functional consequences of HRS governance over WASH recruitment by showing a requirement for HRS in the constitutive recycling of the WASH dependent cargos EGFR, ci-M6PR and MT1-MMP. The HRS/WASH axis facilitated recycling of EGFR and MT1-MMP through a mechanism that required direct Actin binding of the receptors at the endosome. This introduces a new principle for sequence dependent sorting at the endosome which may extend to other recycling components known to be able to indirectly interact with Actin such as Integrins (Calderwood et al., 2000; Jiang et al., 2003). Previously Actin on endosomes has been shown to provide a mode for stabilising tubules, allowing more time for receptors to be concentrated (Puthenveedu et al., 2010). Whilst the WASH complex binds to the fission machinery through Dynamin for the pinching off of new vesicles from the sorting endosome (Derivery et al., 2009), we propose that endosomal F-Actin function could include sequestering receptors into discrete recycling subdomains on the limiting membrane, concentrating receptors and enabling their efficient recycling (Fig. 9) (Puthenveedu et al., 2010; Zech et al., 2012). This hypothesis is supported by our chimera experiments using a Transferrin receptor scaffold, where the inclusion of the Actin binding domain from MT1-MMP could overcome ubiquitin mediated sorting by the ESCRT complex (Raiborg et al., 2002). These three levels of Actin involvement on the endosome provide a coherent set of steps that require Actin involvement in receptor trafficking, from cargo sorting to fission of the vesicle on a recycling ready endosome.

How can we reconcile the fact that EGFR ubiquitylation provides a signal for degradation, yet it incorporates an Actin-binding motif that can deflect from this pathway? Our chimera experiments are conducted with a single ubiquitin moiety providing the lysosomal sorting signal. In reality acutely activated EGF receptors are decorated with multiple ubiquitin molecules through mono-

ubiquitylation and ubiquitin chains (Huang et al., 2006). Thus, we propose that under steady state conditions, where EGFR is internalized but not tagged for degradation, the Actin-binding motif may ensure efficient recycling and/or deposition at a specific area of the plasma membrane. Under conditions of strong acute stimulation that lead to receptor degradation the co-operativity of multiple ubiquitin interactions within the ESCRT-0 and -I complexes may ensure that the ESCRT/MVB pathway is engaged to a larger extend.

However, a central conundrum remains, in that both opposing pathways require receptor interactions with HRS. It is possible that the VHS domain of HRS, like its equivalent in GGA proteins, can bind to both ubiquitylated and non-ubiquitylated proteins, since binding has only ever been tested with ubiquitylated proteins (Ren and Hurley, 2010). Another possibility invokes the enigmatic function of the phosphorylation of HRS (Row et al., 2005). HRS was originally identified as a prominent substrate of receptor tyrosine kinases (Komada and Kitamura, 1995). It could be that following engagement of activated receptors, the consequent HRS phosphorylation disables the recycling function of HRS by its removal from the endomembrane (Urbe et al., 2000), in order to ensure effective degradation.

Cancer cell invasion is dependent on recycling of proteins required for matrix degradation and interactions (Castro-Castro et al., 2016; Caswell and Norman, 2008). We found that HRS and Actin binding of MT1-MMP are necessary for recycling of MT1-MMP. We have demonstrated the functional importance of this axis by the blockade in breast cancer cell invasion with loss of HRS/WASH. Depletion of HRS function did not result in changes in random migration on two-dimensional substrates, thus the basic migration machinery of the cell remains intact. In contrast, invasion into 3D collagen organotypic raft culture and the associated ability of cells to degrade matrix was abrogated. The invasive migration of triple negative MDA-MB-231 breast cancer cells through dense matrix, has been shown to depend on the function and localization of MT1-MMP in invasive pseudopods (Castro-Castro et al., 2016; Monteiro et al., 2013). We propose that failure of MT1-MMP recycling when HRS/WASH are lost explains this loss of invasive capability with intact migration capacity demonstrating the functional importance of this axis in invasive migration.

## Materials and Methods

### Materials

The following antibodies were used in the study for (specific applications indicated where two antibodies against the same target are noted) anti-EEA1 (BD #610457), anti-EGFR (BD #555996) (recycling assays), anti-EGFR (CST #4267)(IF), anti-EGFR (Abcam #ab52894) (rabbit IF), anti-p34 (Millipore 07-227), anti-Cathepsin D (Calbiochem 219361), CCDC53 (Atlas HPA038338), Strumpellin (Millipore, ab101222), MT1-MMP antibody (Millipore, MAB3328), anti-VPS35 (Abcam #Ab10099), anti-WASH (ATLAS #HPA002689), anti-HRS (Everest #EBO7211) (WB), anti-HRS ( ALX-804-382-C050) (IF), anti-STAM (Homemade (Row et al., 2005)), anti-CCDC53 (Millipore #ABT69), anti-Myc (Merek #05-274), anti-ciM6PR (Abcam #ab2733), anti-TGN46 (Sigma #T7576),

COMMD1 (Proteintech 11938-1-AP), rabbit anti-Transferrin receptor (Abcam, #ab84036), mouse anti-transferrin receptor (Abcam #ab38171), anti-α-Tubulin (Sigma #T5168) anti-GAPDH (Millipore #AB2302). Donkey IR700 and IR800-coupled anti-mouse and anti-rabbit secondary antibodies were purchased from LI-COR and AlexaFluor-488, AlexaFluor 594 and AlexaFluor 647-coupled donkey anti-mouse, anti-goat and anti-rabbit antibodies were obtained from Molecular Probes. Acti-stain 670 phalloidin (Cytoskeleton, Inc.). FITC-Trf (Molecular Probes, #T2871).

The following siRNA was used in this study, NT: Allstar negative non-targeting control 2 (Qiagen), WASH-1:GCCACAGGAUCCAGAGCAA(dTdT), HRS-1:CGUCUUUCCAGAAUUCAAA(dTdT) (Ambion ID:s17480), HRS-2:UGGAAUCUGUGGUAAAGAA(dTdT)(Ambion ID:s17481). MT1-MMP: GACAGCGGTCTAGGAATTCAA

All other reagents were acquired from SIGMA unless otherwise stated.

**Cell culture and transfection**

HeLa, HeLa S3 (Flp-in) and MDA-MB-231 cells were cultured at 37°C in 5% $CO_2$ in Dulbecco's Modified Eagle's' Medium (DMEM) supplemented with 10% FBS (fetal bovine serum), 1% nonessential amino acids and 1% penicillin/streptomycin sulphate. Flp-In$^{TM}$ HeLa S3 cells stably transfected cells were supplemented with 150µg/ml Hygromycin B. For siRNA transfections all cells were treated with siRNA to a final concentration of 50nM twice over 120 hours at 0 and 48 hour time points. HeLa and HeLa S3 (Flp-In cells were treated using RNAiMAX transfection reagent (Invitrogen), MDA-MB-231 cells were treated using Lullaby transfection reagent (OZ bioscience). For plasmid expression all cells were transfected using Lipofectamine 2000 in a ratio of 1µg DNA:3µl Lipofectamine 2000 for one well of a six well plate.

**Generating stable cell lines**

A Flp-In HeLa S3 stable host cell line was generated according to the Flp-In$^{TM}$ system manufacturer's (Invitrogen) instructions and verified by Northern blotting (data not shown). GFP and GFP-HRS were amplified from pEGFP-C1-HRS (mouse) with the following primers: forward, both with 5'-CACCATGGTGAGCAAGGGCG; reverse, GFP with 5'-TTAGGATCTGAGTCCGGACTTGTACAGC and GFP-HRS with 5'-GGCCCGCGGTACCGTCGA. PCR products were then cloned into pEF5/FRT/V5 TOPO using pEF5/FRT/V5 Directional TOPO® Cloning Kit (Life technologies), resulting in pEF5/FRT/V5 -GFP and pEF5/FRT/V5 -GFP-HRS plasmids. To generate stable cell lines, HeLa S3 Flp-In host cells were transfected with pEF5/FRT/V5 -GFP, pEF5/FRT/V5 -GFP-HRS together with pOG44 plasmid which expresses the Flp recombinase at a ratio of 1:9. Following Hygromycin B selection (200µg/ml), single colonies were picked and grown up separately as individual clones.

**Microscopy**

Cells for regular Immunofluorescence were fixed in 4%PFA/PBS, quenched in 50mM $NH_4Cl$, permeabilised in 0.2% Triton-X100/PBS, blocking and antibody labelling was performed in 5% donkey serum. For Guanidinium Hydrochloride denaturing based staining the same protocol was followed with the addition of ten minutes incubation in 6M Guanidinium Hydrochloride followed by three washes in PBS after permeabilization. All images were recorded with a Marianas spinning disk confocal microscope (3i) using a 63x 1.4NA or 10× 0.45NA Zeiss Plan-Apochromat lens and either an Evolve EMCCD (Photometrics) or FLASH4 sCMOS (Hamamatsu) camera or Zeiss LSM800 with Airyscan module, using a 63x 1.4NA Zeiss Plan-Apochromat. Single cell migration assays were performed on a Nikon Ti-E using a 20x CFI Super plan Fluor ELWD ADM 0.45NA and a CoolSnap HQ camera (Photometrics).

paCherry and paGFP experiments were performed by exposure of Rab4 or EEA1 positive endosomes to a brief pulse of 405nm laser light. A time sequence was acquired. The intensity of fluorescence in the endosome was quantified and normalised to background photo-bleaching and peak endosomal fluorescence. Rate of decay of fluorescence ($k=sec^{-1}$) was extracted from curves fitted using one phase dissociation equation in GraphPad prism. For FRAP experiments a one phase association curve was fitted to the data and the rate constant $k=sec^{-1}$ was extracted. Slidebook software (3i) was used to quantify co-localization, FRAP and paGFP photo activation experiments. Zeiss Zen software was used to process Airyscan images and ImageJ FRAPprofiler plugin was used to quantify paCherry photo activation experiments. For WASH/EEA1 in Flp-In cells, EGFR/EEA1, VPS35/EEA1, a mask was generated around EEA1 or TGN46 positive structures, the background was subtracted and the co-localisation of EEA1 and WASH was calculated as Pearson R value (R). For ciM6PR experiments co-localisation was calculated from the whole cell using either slidebook software of ImageJ. SUM intensity measurements on endosomes was quantified by making a mask around the endosome (EEA1 or VPS35) then calculating the SUM intensity using the slidebook software in the endosome divided by the volume of the endosome. Calculation of co-localisation with EEA1 (GFP-VHS-FYVE rescue experiments and HRS rescue experiments) was performed by generating a mask around EEA1 calculating the Pearson's R value in slidebook. Thresholds were set the same for all images. For TrfR recycling assay a mask was generated around Myc-TrfR signal and the R value against Trf-488 was measured. For Actin quantification on endosomes a mask was generated around VPS35 positive structures and the intensity of Actin was measured in the mask. Single cell tracking was analysed using the manual tracking and chemotaxis plugin in ImageJ. Identical exposure settings where used in all experiments where comparisons were made between conditions.

**Proximity Ligation assay (PLA)**

HeLa S3 cell were seeded on coverslips 24 hours prior to assay. Cells were fixed with 4% PFA and permeabilised with 0.2% Triton-X100/PBS. Proximity ligation assays was carried out using the

Duolink II reagent kit (Olink) according to manufacturers specifications using blocking buffers and antibody diluent outlined above (see microscopy), HRS and WASH antibodies were used at a dilution factor of 1:500. Either HRS or WASH antibodies alone were used as technical controls. Coverslips were imaged using the Marianas spinning disk confocal microscope (3i), 40x objective lens and FLASH4 sCMOS (Hamamatsu) camera. PLA signals were identified and counted using ImageJ and expressed as the number of signals/cells in the optical field.

**TrfR chimera assays**

Transferrin receptor chimera recycling assay was adapted from Raiborg et al. (Raiborg et al., 2002). TrfR chimera constructs have been previously described (Raiborg et al., 2002). In brief, mouse ubiquitin was fused to human TrfR construct with a spacer Arg-Ser-Gln-Gln and the omission of the carboxy tail glycine residues of ubiquitin to prevent the removal of ubiquitin by deubiquitinases. The Actin binding domain from MT1-MMP was inserted between TrfR tail and Ubiquitin moiety by annealing the following primers:
5'-
TCTCAGAAGATCACAACAGGTCAAGGACCTGCTGTCCCGTCAGTGCTACCTCCTGCGAAGGA
TGATGGAT-3'
5'ATCCATCATCCTTCGCAGGAGGTAGCACTGACGGGACAGCAGGTCCTTGACCTGTTGTGAT
CTTCTGAG-3'
The whole construct was generated by PCR reaction using the following primers and pcDNA3-6-HIS-Ub, pcDNA3-hTrFR vectors generously provided by Dr Raiborg, Centre for Cancer Biomedicine Norwegian Radium Hospital, Oslo, NO.
Ub_F:5'-CT GGA TCC ATG CAG ATC TTC GTG AAG ACT-3'
TrfR:5'-CGT TTG GGA CAT TGA CAA TGA GTT TTA A ACT AGT GAA TTC AT-3'
Ubiquitin-MTMMP1(Tail)fusion
5'- C CTG GTG CTC CGT CTC AGA AGA TCA CAA CAG GTC AAG -3'
5'-CTTGACCTGTTGTGATCTTCTGAGACGGAGCACCAGG-3'
MTMMP1(Tail)-TrfR fusion:
5'- GCTACCTCCTGCGAAGGATGATGGATCAAGCTAGATCAGCA -3'
5'-TGCTGATCTAGCTTGATCCATCATCCTTCGCAGGAGGTAGC-3'
The constructs were then subcloned into pDM734 vector to add a myc tag.

HeLa and HeLaS3 cells were transfected with TrfR constructs for 24 hours before incubation with 50µg/ml FITC-Trf for 15mins. The cells were washed in warm PBS and then allowed to recycle the TrfR construct in fresh full DMEM supplemented with 50µg/ml leupeptin and 100µg/ml cycloheximide. Cells were either fixed in 4% PFA before processing for immunofluorescence or flow cytometry. For analysis by flow cytometry following TrfR construct transfection as described above, cells were serum starved for 1-2 hours before harvesting using 5mM EDTA at 37°C. Cells were washed 3x in PBS and resuspended in serum free medium for incubation on ice for 30

minutes. Cells were then incubated with 37°C full DMEM supplemented with, 50µg/ml FITC-Trf for 30 minutes at 37°C before being returned to ice. Cells were washed 3x with ice cold PBS before incubation in 37°C full DMEM supplemented with 50µg/ml leupeptin and 100µg/ml cycloheximide for the indicated recycling time points. Following incubation cells were returned to ice and washed 3x with ice cold PBS prior to fixation in 4% paraformaldehyde for 30 minutes. Cells were permeabilised with 0.1% Triton-X100 for 15 minutes, washed and blocked with 1% BSA for 15 minutes. To determine the mean fluorescence intensity of FITC-Trf in cells expressing TrfR constructs. Cells were labelled with mouse anti-Myc (Millipore) primary antibody followed by Alexa-594 anti-mouse secondary antibody (Invitrogen). FITC-Trf mean fluorescence intensity of Alexa-594 positive cells was determined using an Attune NxT Flow cytometer (Thermofisher).

**ci-M6PR secretion assay**

Assay was performed as described in (MacDonald et al., 2014). In brief siRNA treated HeLa cells were washed in PBS and incubated overnight in OptiMEM (Gibco, Thermo Fisher). The conditioned media was collected. Protein content was TCA precipitated and the resulting pellet was resuspended in SDS running buffer. The underlying cells were lysed in NP40 buffer.

**EGFR trafficking assays**

The EGFR trafficking assay was performed as previously described in (Roberts et al., 2001). In brief, siRNA treated MDA-MB-231 cells were seeded into 10cm dishes and grown to sub-confluency on the day of the experiment. Cells were serum starved 1 hour prior to recycling in serum free DMEM, cells were then biotinylated on ice in 10mg sulfo-NHS-SS-Biotin/75ml/PBS (Thermo fisher #21331). Cells were then placed in serum free DMEM 37$^{o}$C for 30 minutes to internalise receptor:biotin complexes to equilibrium, remaining cell surface biotin was stripped in 92mM MESNA. Cells were then placed again in serum free DMEM for defined recycling periods at 37°C and subsequently stripped again and quenched with Iodoacetamide. Cells were scraped and syringed in lysis buffer (200mM NaCl, 75mM Tris, 15mM NaF, 7.5mM EDTA, and EGTA, 1.5% Triton-X-100, 0.075% Igepal CA-630 and Halt protease and phosphatase inhibitors (Thermofisher)). The levels of biotinylated receptor were measured using a sandwich ELISA with anti-EGFR antibody, streptavidin-Horseradish peroxidase and 0.56mg/ml ortho-phenylenediamine. The percentage of recycled receptor was quantified as a percentage of the internal pool.

**EGFR cell surface expression**

In brief, following siRNA transfection (120 h) cells were harvested using 5 mM EDTA/PBS at 37°C. Cells were washed 3x in PBS and fixed in 4% paraformaldehyde for 30 minutes, washed and blocked using 2% BSA/PBS supplemented with 0.1% sodium azide for 15 minutes. Cells were labelled with rabbit anti-EGFR primary antibody followed by Alexa-488 anti-rabbit secondary

antibody. Mean fluorescence intensity of Alexa-488 positive cells was determined using an Attune NxT Flow cytometer (Thermofisher).

**Cell lysis for western blotting**

Cells were washed 2x in ice cold PBS and lysed as indicated in NP40 buffer (0.5% NP40, 25 mM Tris pH 7.5, 100 mM NaCl) or RIPA buffer (10mM Tris-HCl, 150mM NaCl, 1% Triton-X100 (w/v), 0.1% (w/v) SDS and 1% (w/v) sodium deoxycholate) supplemented with Halt protease and phosphatase inhibitors (Thermofisher) by rocking at 4$^{o}$C for 10mins.

**Gelatin degradation assay**

siRNA treated MDA-MB-231 cells were seeded for 16 hours onto 488-gelatin covered coverslips. The cells were fixed in 4% PFA/PBS and processed for IF. Degradation was quantified by counting cells that had Actin positive degradation spots below the cell.

**Invasion assays**

Inverted invasion assays were performed as described previously (Hennigan et al., 1994). In brief, Matrigel (Corning) was diluted with PBS to 5mg/ml, supplemented with fibronectin to a final concentration of 25µg/ml and polymerised in transwell inserts (Corning) at 37°C for 1 hour. Inserts were inverted and 8 x $10^4$ cells were seeded directly to the bottom of the filter. MDA-MB-231 cells were seeded and allowed to adhere for 3-6 hours. Once adhered the inserts were turned right-side-up. Serum-free medium was added to the wells of the transwell plate, and medium supplemented with 10% FBS and 20 ng/ml EGF was added on top of the Matrigel. Following 5 days incubation gels were fixed in 4% paraformaldehyde for 30 min, followed by permeabilization with 0.1% Triton-X100 in PBS for 30 min. Samples were then stained with DAPI (Sigma) for 1 hour or overnight at 4°C. Cells failing to cross the filter were removed with tissue. Serial optical sections of the plug at 10 µm intervals using an inverted spinning disk confocal microscope (Marianas, 3i) fitted with a 10×0.45NA air objective lens were taken. ImageJ was used to determine the integrated density of each optical section to determine the invasion (Invasion index = (∑ integrated density of 1st 30µM)/ (∑ integrated density of invasion)) and expressed as fold change with respect to the NT control as performed in (Zech et al., 2011).

Organotypic raft cultures were previously described (Timpson et al., 2011). In brief, at 4°C Immortalised human mammary fibroblasts (8 x $10^4$ /ml) were resuspended in Type 1 rat tail collagen (~1mg/ml) supplemented with 10% FBS, 1x DMEM, pH 7.2 and plated into 35mm dishes (2.5ml/dish). Collagen was allowed to polymerise for 15-30 min and 37°C before adding 1-2 ml of full DMEM Supplemented with HEPES. Media was changed every other day until collagen

contracted to ~1.5cm in diameter. Once contracted, gels were placed into a 24 well plate followed by $7x10^5$ cells in suspension. Cells were allowed to adhere for 3 days, after which gels were lifted onto stainless steel grids in 6 cm dishes. Media supplemented with 20ng/ml EGF was added so the bottom of the gel is in contact with media but not submerged. For negative invasion controls GM6001 (5µM) was added to the media. Following 5 days incubation Gels were cut in half and fixed in 4% paraformaldehyde overnight prior to embedding, sectioning and haematoxylin and eosin staining. Invasion index was determined as previously described (Invasion index = mean invasive depth x number of particles x area of particles) (Jenei et al., 2011).

**Online supplemental material**

Figures S1 and S2 show additional evidence that HRS is required for the endosomal recruitment of WASH and investigate expression levels and localization of associated proteins. Fig. S3 shows evidence that the HRS VHS-FYVE domains are sufficient to recruit WASH to endomembranes. Fig. S4 shows that HRS is required for ci-M6PR receptor recycling. Fig. S5 Shows that loss of HRS does not affect cell migration on a 2D substrate. Video 1. Shows Hela S3 Flp-in cells stably expressing GFP-mHRS, transfected with mCherry-mWASH on a WASH depleted background. Video 2. Photoactivation of endosomal paGFP-EGFR in HRS depleted cells. HeLa cells treated with the indicated siRNA for 120 hours were transfected with paGFP-EGFR and mCherry-RAB4. paGFP was activated in mCherry positive endosomes using a pulse of 405nm laser light. Video 3. Photoactivation of endosomal paGFP-EGFR. HeLa cells were transfected with paGFP-EGFR/paGFP-EGFR-YLIP/AAAA (actin binding mutant) and mCherry-RAB4. paGFP was activated in RAB4 positive endosomes using a pulse of 405nm laser light. Video 4. Cellular distribution of wildtype and actin binding mutant overexpressed GFP-EGFR. HeLa cells transfected with either GFP-EGFR or GFP-EGFR-YLIP/AAAA and mRFP-EEA1. Video 5. HeLa cells transfected with indicated siRNA for 120 hours were transfected with paGFP-EGFR and mCherry-RAB4. Cells were pretreated with 100mM Primaquine to inhibit recycling before paGFP was activated in mCherry positive endosomes using a pulse of 405nm laser light. Video 6. Photoactivation of endosomal paCherry-MT1-MMP constructs. MDA-MB-231 cells were transfected with paCherry-MT1-MMP/ paCherry-MT1-MMP-LLY/AAA (actin binding mutant) and GFP-EEA1. paCherry was activated in EEA1 positive endosomes using a pulse of 405nm laser light.

**Acknowledgments**

The authors would like to thank Laura Machesky, Camilla Raiborg, Emmanuel Derivery, Alexis Gautreau, Mark Morgan and Philippe Chavrier for their generous provision of reagents, Liverpool BIO-Innovation hub (LBIH) BIOBANK for sectioning of organotypic cultures, Institute of Translational Medicine Biomedical imaging facility and Cesar Augusto Valades Cruz for advice on image anaylsis. EM was funded by a North West Cancer Research grant to TZ, LB is funded by a Breast Cancer Now grant to TZ. DN and DG are supported by a Wellcome Trust PhD studentship

and TW by DiMeN BBSRC doctoral training program. The authors declare no competing financial interests.

**Author contributions**

EM performed the majority of experiments and co-wrote the manuscript. LB, AS, TW, DN, DG and JB performed experiments. HL, MC and SU generated and verified the stable GFP-mHRS cell lines and critically read the manuscript. TZ performed experiments and co-wrote the manuscript.

**Bibliography**

Apodaca, G., L.A. Katz, and K.E. Mostov. 1994. Receptor-mediated transcytosis of IgA in MDCK cells is via apical recycling endosomes. *J Cell Biol*. 125:67-86.

Bache, K.G., A. Brech, A. Mehlum, and H. Stenmark. 2003. Hrs regulates multivesicular body formation via ESCRT recruitment to endosomes. *J Cell Biol*. 162:435-442.

Barbieri, M.A., G.P. Li, L.S. Mayorga, and P.D. Stahl. 1996. Characterisation of rab5-Q79L-stimulated endosome fusion. *Arch. Biochem. Biophys.* 326:64-72.

Bartuzi, P., D.D. Billadeau, R. Favier, S. Rong, D. Dekker, A. Fedoseienko, H. Fieten, M. Wijers, J.H. Levels, N. Huijkman, N. Kloosterhuis, H. van der Molen, G. Brufau, A.K. Groen, A.M. Elliott, J.A. Kuivenhoven, B. Plecko, G. Grangl, J. McGaughran, J.D. Horton, E. Burstein, M.H. Hofker, and B. van de Sluis. 2016. CCC- and WASH-mediated endosomal sorting of LDLR is required for normal clearance of circulating LDL. *Nat Commun*. 7:10961.

Calderwood, D.A., S.J. Shattil, and M.H. Ginsberg. 2000. Integrins and actin filaments: reciprocal regulation of cell adhesion and signaling. *J Biol Chem*. 275:22607-22610.

Carnell, M., T. Zech, S.D. Calaminus, S. Ura, M. Hagedorn, S.A. Johnston, R.C. May, T. Soldati, L.M. Machesky, and R.H. Insall. 2011. Actin polymerization driven by WASH causes V-ATPase retrieval and vesicle neutralization before exocytosis. *J Cell Biol*. 193:831-839.

Castro-Castro, A., V. Marchesin, P. Monteiro, C. Lodillinsky, C. Rosse, and P. Chavrier. 2016. Cellular and Molecular Mechanisms of MT1-MMP-Dependent Cancer Cell Invasion. *Annu Rev Cell Dev Biol*. 32:555-576.

Caswell, P., and J. Norman. 2008. Endocytic transport of integrins during cell migration and invasion. *Trends Cell Biol*. 18:257-263.

Caswell, P.T., M. Chan, A.J. Lindsay, M.W. McCaffrey, D. Boettiger, and J.C. Norman. 2008. Rab-coupling protein coordinates recycling of alpha5beta1 integrin and EGFR1 to promote cell migration in 3D microenvironments. *J Cell Biol*. 183:143-155.

Clague, M., and S. Urbe. 2003. Hrs function: viruses provide the clue. *Trends in Cell Biology*. 13:603-606.

den Hartigh, J.C., P.M. van Bergen en Henegouwen, A.J. Verkleij, and J. Boonstra. 1992. The EGF receptor is an actin-binding protein. *J Cell Biol*. 119:349-355.

Derivery, E., C. Sousa, J.J. Gautier, B. Lombard, D. Loew, and A. Gautreau. 2009. The Arp2/3 activator WASH controls the fission of endosomes through a large multiprotein complex. *Dev Cell*. 17:712-723.

Dozynkiewicz, M.A., N.B. Jamieson, I. Macpherson, J. Grindlay, P.V. van den Berghe, A. von Thun, J.P. Morton, C. Gourley, P. Timpson, C. Nixon, C.J. McKay, R. Carter, D. Strachan, K. Anderson, O.J. Sansom, P.T. Caswell, and J.C. Norman. 2012. Rab25 and CLIC3 collaborate to promote integrin recycling from late endosomes/lysosomes and drive cancer progression. *Dev Cell*. 22:131-145.

Dupont, S., L. Morsut, M. Aragona, E. Enzo, S. Giulitti, M. Cordenonsi, F. Zanconato, J. Le Digabel, M. Forcato, S. Bicciato, N. Elvassore, and S. Piccolo. 2011. Role of YAP/TAZ in mechanotransduction. *Nature*. 474:179-183.

Gomez, T.S., and D.D. Billadeau. 2009. A FAM21-containing WASH complex regulates retromer-dependent sorting. *Dev Cell*. 17:699-711.

Gomez, T.S., J.A. Gorman, A.A. de Narvajas, A.O. Koenig, and D.D. Billadeau. 2012. Trafficking defects in WASH-knockout fibroblasts originate from collapsed endosomal and lysosomal networks. *Mol Biol Cell*. 23:3215-3228.

Gruenberg, J. 2001. The endocytic pathway: a mosaic of domains. *Nat Rev Mol Cell Biol*. 2:721-730.

Hanyaloglu, A.C., and M. von Zastrow. 2007. A novel sorting sequence in the beta2-adrenergic receptor switches recycling from default to the Hrs-dependent mechanism. *J Biol Chem*. 282:3095-3104.

Hao, Y.H., J.M. Doyle, S. Ramanathan, T.S. Gomez, D. Jia, M. Xu, Z.J. Chen, D.D. Billadeau, M.K. Rosen, and P.R. Potts. 2013. Regulation of WASH-dependent actin polymerization and protein trafficking by ubiquitination. *Cell*. 152:1051-1064.

Hao, Y.H., M.D. Fountain, Jr., K. Fon Tacer, F. Xia, W. Bi, S.H. Kang, A. Patel, J.A. Rosenfeld, C. Le Caignec, B. Isidor, I.D. Krantz, S.E. Noon, J.P. Pfotenhauer, T.M. Morgan, R. Moran, R.C. Pedersen, M.S. Saenz, C.P. Schaaf, and P.R. Potts. 2015. USP7 Acts as a Molecular Rheostat to Promote WASH-Dependent Endosomal Protein Recycling and Is Mutated in a Human Neurodevelopmental Disorder. *Mol Cell*. 59:956-969.

Harbour, M.E., S.Y. Breusegem, R. Antrobus, C. Freeman, E. Reid, and M.N. Seaman. 2010. The cargo-selective retromer complex is a recruiting hub for protein complexes that regulate endosomal tubule dynamics. *J Cell Sci*. 123:3703-3717.

Harbour, M.E., S.Y. Breusegem, and M.N. Seaman. 2012. Recruitment of the endosomal WASH complex is mediated by the extended 'tail' of Fam21 binding to the retromer protein Vps35. *Biochem J*. 442:209-220.

Helfer, E., M.E. Harbour, V. Henriot, G. Lakisic, C. Sousa-Blin, L. Volceanov, M.N. Seaman, and A. Gautreau. 2013. Endosomal recruitment of the WASH complex: active sequences and mutations impairing interaction with the retromer. *Biol Cell*. 105:191-207.

Henne, W.M., N.J. Buchkovich, and S.D. Emr. 2011. The ESCRT pathway. *Dev Cell*. 21:77-91.

Hennigan, R.F., K.L. Hawker, and B.W. Ozanne. 1994. Fos-transformation activates genes associated with invasion. *Oncogene*. 9:3591-3600.

Hotary, K., X.Y. Li, E. Allen, S.L. Stevens, and S.J. Weiss. 2006. A cancer cell metalloprotease triad regulates the basement membrane transmigration program. *Genes Dev*. 20:2673-2686.

Hotary, K.B., E.D. Allen, P.C. Brooks, N.S. Datta, M.W. Long, and S.J. Weiss. 2003. Membrane type I matrix metalloproteinase usurps tumor growth control imposed by the three-dimensional extracellular matrix. *Cell*. 114:33-45.

Huang, F., D. Kirkpatrick, X. Jiang, S. Gygi, and A. Sorkin. 2006. Differential regulation of EGF receptor internalization and degradation by multiubiquitination within the kinase domain. *Mol Cell*. 21:737-748.

Huang, S.H., L. Zhao, Z.P. Sun, X.Z. Li, Z. Geng, K.D. Zhang, M.V. Chao, and Z.Y. Chen. 2009. Essential role of Hrs in endocytic recycling of full-length TrkB receptor but not its isoform TrkB.T1. *J Biol Chem*. 284:15126-15136.

Jenei, V., M.L. Nystrom, and G.J. Thomas. 2011. Measuring invasion in an organotypic model. *Methods Mol Biol*. 769:223-232.

Jia, D., T.S. Gomez, D.D. Billadeau, and M.K. Rosen. 2012. Multiple repeat elements within the FAM21 tail link the WASH actin regulatory complex to the retromer. *Mol Biol Cell*. 23:2352-2361.

Jia, D., T.S. Gomez, Z. Metlagel, J. Umetani, Z. Otwinowski, M.K. Rosen, and D.D. Billadeau. 2010. WASH and WAVE actin regulators of the Wiskott-Aldrich syndrome protein (WASP) family are controlled by analogous structurally related complexes. *Proc Natl Acad Sci U S A*. 107:10442-10447.

Jiang, G., G. Giannone, D.R. Critchley, E. Fukumoto, and M.P. Sheetz. 2003. Two-piconewton slip bond between fibronectin and the cytoskeleton depends on talin. *Nature*. 424:334-337.

Jing, S.Q., T. Spencer, K. Miller, C. Hopkins, and I.S. Trowbridge. 1990. Role of the human transferrin receptor cytoplasmic domain in endocytosis: localization of a specific signal sequence for internalization. *J Cell Biol*. 110:283-294.

Komada, M., and N. Kitamura. 1995. Growth-factor-induced tyrosine phosphorylation of hrs, a novel 115-kilodalton protein with a structurally conserved putative zinc finger domain. *Mol. Cell Biol.* 15:6213-6221.

Lauwers, E., C. Jacob, and B. Andre. 2009. K63-linked ubiquitin chains as a specific signal for protein sorting into the multivesicular body pathway. *J Cell Biol*. 185:493-502.

Lobel, P., K. Fujimoto, R.D. Ye, G. Griffiths, and S. Kornfeld. 1989. Mutations in the cytoplasmic domain of the 275 kd mannose 6-phosphate receptor differentially alter lysosomal enzyme sorting and endocytosis. *Cell*. 57:787-796.

Luini, A., A. Ragnini-Wilson, R.S. Polishchuck, and M.A. De Matteis. 2005. Large pleiomorphic traffic intermediates in the secretory pathway. *Curr Opin Cell Biol*. 17:353-361.

MacDonald, E., S. Urbe, and M.J. Clague. 2014. USP8 controls the trafficking and sorting of lysosomal enzymes. *Traffic*. 15:879-888.

Macpherson, I.R., E. Rainero, L.E. Mitchell, P.V. van den Berghe, C. Speirs, M.A. Dozynkiewicz, S. Chaudhary, G. Kalna, J. Edwards, P. Timpson, and J.C. Norman. 2014. CLIC3 controls recycling of late endosomal MT1-MMP and dictates invasion and metastasis in breast cancer. *J Cell Sci*. 127:3893-3901.

Mao, Y., A. Nickitenko, X. Duan, T.E. Lloyd, M.N. Wu, H. Bellen, and F.A. Quiocho. 2000. Crystal structure of the VHS and FYVE tandem domains of Hrs, a protein involved in membrane trafficking and signal transduction. *Cell*. 100:447-456.

Matter, K., and I. Mellmann. 1994. Mechanisms of cell polarity: sorting and transport in epithelial cells. *Curr. Op. Cell Biol.* 6:545-554.

Mayor, S., J.F. Presley, and F.R. Maxfield. 1993. Sorting of membrane-components from endosomes and subsequent recycling to the cell-surface occurs by a bulk flow process. *J. Cell Biol.* 121:1257-1269.

McNally, K.E., R. Faulkner, F. Steinberg, M. Gallon, R. Ghai, D. Pim, p. Langton, N. Pearson, C.M, Danson, H. Nägele, L.L. Morris, A. Singla, B.L.Overlee, K.J. Heesom, R. Sessions, L. Banks, B.M. Collins, I. Berger, D.D. Billadeau, E. Berstein, P.J. Cullen. 2017. Retriever is a multiprotein complex for retromer-independent endosomal cargo recycling. *Nat Cell Biol.* 19(10):1214-1225

Misra, S., R. Puertollano, Y. Kato, J.S. Bonifacino, and J.H. Hurley. 2002. Structural basis for acidic-cluster-dileucine sorting-signal recognition by VHS domains. *Nature*. 415:933-937.

Monteiro, P., C. Rosse, A. Castro-Castro, M. Irondelle, E. Lagoutte, P. Paul-Gilloteaux, C. Desnos, E. Formstecher, F. Darchen, D. Perrais, A. Gautreau, M. Hertzog, and P. Chavrier. 2013. Endosomal WASH and exocyst complexes control exocytosis of MT1-MMP at invadopodia. *J Cell Biol*. 203:1063-1079.

Park, L., P.A.Thomason, T.Zech, J.S.King, D.M.Veltman, M,Carnell, S. Ura, L.M. Machesky, R.M. Insall. 2013. Cyclical action of the WASH complex: FAM21 and capping protein drive WASH recycling, not initial recruitment. *Dev Cell. 24(2):169-81.*

Pons, V., P.P. Luyet, E. Morel, L. Abrami, F.G. van der Goot, R.G. Parton, and J. Gruenberg. 2008. Hrs and SNX3 functions in sorting and membrane invagination within multivesicular bodies. *PLoS Biol*. 6:e214.

Popoff, V., G.A. Mardones, S.K. Bai, V. Chambon, D. Tenza, P.V. Burgos, A. Shi, P. Benaroch, S. Urbe, C. Lamaze, B.D. Grant, G. Raposo, and L. Johannes. 2009. Analysis of articulation between clathrin and retromer in retrograde sorting on early endosomes. *Traffic*. 10:1868-1880.

Pornillos, O., D.S. Higginson, K.M. Stray, R.D. Fisher, J.E. Garrus, M. Payne, G.P. He, H.E. Wang, S.G. Morham, and W.I. Sundquist. 2003. HIV Gag mimics the Tsg101-recruiting activity of the human Hrs protein. *J Cell Biol*. 162:425-434.

Puertollano, R., R.C. Aguilar, I. Gorshkova, R.J. Crouch, and J.S. Bonifacino. 2001. Sorting of mannose 6-phosphate receptors mediated by the GGAs. *Science*. 292:1712-1716.

Puthenveedu, M.A., B. Lauffer, P. Temkin, R. Vistein, P. Carlton, K. Thorn, J. Taunton, O.D. Weiner, R.G. Parton, and M. von Zastrow. 2010. Sequence-dependent sorting of recycling proteins by actin-stabilized endosomal microdomains. *Cell*. 143:761-773.

Raiborg, C., K.G. Bache, D.J. Gillooly, I.H. Madshus, E. Stang, and H. Stenmark. 2002. Hrs sorts ubiquitinated proteins into clathrin-coated microdomains of early endosomes. *Nat Cell Biol*. 4:394-398.

Raiborg, C., B. Bremnes, A. Mehlum, D.J. Gillooly, A. D'Arrigo, E. Stang, and H. Stenmark. 2001. FYVE and coiled-coil domains determine the specific localisation of Hrs to early endosomes. *J Cell Sci*. 114:2255-2263.

Ren, X., and J.H. Hurley. 2010. VHS domains of ESCRT-0 cooperate in high-avidity binding to polyubiquitinated cargo. *EMBO J*. 29:1045-1054.

Roberts, M., S. Barry, A. Woods, P. van der Sluijs, and J. Norman. 2001. PDGF-regulated rab4-dependent recycling of alphavbeta3 integrin from early endosomes is necessary for cell adhesion and spreading. *Curr Biol*. 11:1392-1402.

Row, P.E., M.J. Clague, and S. Urbe. 2005. Growth factors induce differential phosphorylation profiles of the Hrs-STAM complex: a common node in signalling networks with signal-specific properties. *Biochem J*. 389:629-636.

Sabeh, F., I. Ota, K. Holmbeck, H. Birkedal-Hansen, P. Soloway, M. Balbin, C. Lopez-Otin, S. Shapiro, M. Inada, S. Krane, E. Allen, D. Chung, and S.J. Weiss. 2004. Tumor cell traffic through the extracellular matrix is controlled by the membrane-anchored collagenase MT1-MMP. *J Cell Biol*. 167:769-781.

Sigismund, S., V. Algisi, G. Nappo, A. Conte, R. Pascolutti, A. Cuomo, T. Bonaldi, E. Argenzio, L.G. Verhoef, E. Maspero, F. Bianchi, F. Capuani, A. Ciliberto, S. Polo, P.P. Di Fiore. 2013. Threshold-controlled ubiquitination of the EGFR directs receptor fate. *EMBO J.* 32(15):2140-57.

Steffen, A., G. Le Dez, R. Poincloux, C. Recchi, P. Nassoy, K. Rottner, T. Galli, and P. Chavrier. 2008. MT1-MMP-dependent invasion is regulated by TI-VAMP/VAMP7. *Curr Biol*. 18:926-931.

Steinberg, F., M. Gallon, M. Winfield, E.C. Thomas, A.J. Bell, K.J. Heesom, J.M. Tavare, and P.J. Cullen. 2013. A global analysis of SNX27-retromer assembly and cargo specificity reveals a function in glucose and metal ion transport. *Nat Cell Biol*. 15:461-471.

Timpson, P., E.J. McGhee, Z. Erami, M. Nobis, J.A. Quinn, M. Edward, and K.I. Anderson. 2011. Organotypic collagen I assay: a malleable platform to assess cell behaviour in a 3-dimensional context. *J Vis Exp*:e3089.

Urbe, S., I.G. Mills, H. Stenmark, N. Kitamura, and M.J. Clague. 2000. Endosomal localization and receptor dynamics determine tyrosine phosphorylation of hepatocyte growth factor-regulated tyrosine kinase substrate. *Mol Cell Biol*. 20:7685-7692.

van Weert, A.W., H.J. Geuze, B. Groothuis, and W. Stoorvogel. 2000. Primaquine interferes with membrane recycling from endosomes to the plasma membrane through a direct interaction with endosomes which does not involve neutralisation of endosomal pH nor osmotic swelling of endosomes. *Eur J Cell Biol*. 79:394-399.

Williams, R.L., and S. Urbe. 2007. The emerging shape of the ESCRT machinery. *Nat Rev Mol Cell Biol*. 8:355-368.

Wolf, K., S. Alexander, V. Schacht, L.M. Coussens, U.H. von Andrian, J. van Rheenen, E. Deryugina, and P. Friedl. 2009. Collagen-based cell migration models in vitro and in vivo. *Semin Cell Dev Biol*. 20:931-941.

Wolf, K., and P. Friedl. 2009. Mapping proteolytic cancer cell-extracellular matrix interfaces. *Clin Exp Metastasis*. 26:289-298.

Yu, X., T. Zech, L. McDonald, E.G. Gonzalez, A. Li, I. Macpherson, J.P. Schwarz, H. Spence, K. Futo, P. Timpson, C. Nixon, Y. Ma, I.M. Anton, B. Visegrady, R.H. Insall, K. Oien, K. Blyth, J.C. Norman, and L.M. Machesky. 2012. N-WASP coordinates the delivery and F-actin-mediated capture of MT1-MMP at invasive pseudopods. *J Cell Biol*. 199:527-544.

Zech, T., S.D. Calaminus, P. Caswell, H.J. Spence, M. Carnell, R.H. Insall, J. Norman, and L.M. Machesky. 2011. The Arp2/3 activator WASH regulates alpha5beta1-integrin-mediated invasive migration. *J Cell Sci*. 124:3753-3759.

Zech, T., S.D. Calaminus, and L.M. Machesky. 2012. Actin on trafficking: could actin guide directed receptor transport? *Cell Adh Migr*. 6:476-481.

Figure 1. HRS is required for the endosomal recruitment of WASH.

A. HeLa cells were treated with the indicated siRNA over 120 hours before fixation in 4%PFA/PBS and labelling with antibodies targeting HRS and WASH. Maximum projection images. B. Airyscan single confocal slice images of HeLa cells fixed and labelled for WASH and HRS. C&D. Proximity Ligation Assay (PLA) of HeLa cells probed for both HRS and WASH or technical single WASH or HRS antibody controls. Data represented as average number of signals per cell. Maximum projection images (nuclei stained with DAPI). (scale bar 20µm, n=3, error bars = STD err). E&F. HeLa S3 Flp-In cells stably transfected with GFP-HRS (mouse) were treated with siRNA targeting endogenous HRS over 120 hours before fixation in 4%PFA/PBS or lysis in NP40 buffer. Single confocal slice images. G. Quantification of Pearson R correlation between EEA1 and WASH (n=3, error bars = STD err, >150 cells total). H&I. HeLa cells were treated with siRNA over 120 hours before fixation in 4%PFA/PBS and labelling with antibodies targeting EEA1 and 647-Phalloidin. Quantfication of sum intensity of actin on endosome. Maximum projection images. (n=3, error bars = STD err, >30 cells total). Statistical analysis = One-way ANOVA, Dunnett's post test.
Scale bar = 10µm.

Figure 2. HRS is required for the endosomal recruitment of WASH independent of VPS35.

A. HeLa cells were treated with the indicated siRNA over 120 hours before fixation in 4%PFA/PBS and labelling with antibodies targeting VPS35 and EEA1. Single confocal slice images. B. Pearson's R correlation value between VPS35 and EEA1 (10 images per condition, >150 cells

total). C. Relative intensity of VPS35 on EEA1 positive endosomes normalised to endosome size (n=3, error bars = STD err, >150 cells total). D. HeLa cells were depleted for HRS over 120 hours before transfection with mCherry-WASH construct 24 hours before imaging; the cells were subjected to photobleaching with a 594nm laser. Fluorescence recovery was measured using the FRAP tool in the slidebook image analysis suite. E. The rate constants ($k=sec^{-1}$) for the recovery curves were extracted using Graphpad prism, the average rate constants of 3 independent experiments is plotted (n=3, error bars = STD err, > 10 cells per condition per experiment). F. HeLa cells were depleted of HRS with siRNA over 120 hours before transfection with YFP-VPS35 construct 24 hours before imaging, Cells were incubated with 647-dextran for 15mins before imaging to mark the endocytic network and YFP-VPS35 positive endosomes were subjected to photobleaching with 594nm laser light. G. The rate constants ($k=sec^{-1}$) for the recovery curves were extracted using graphpad prism, the average rate constants of 3 independent experiments is ploted (n=3, error bars = STD err, > 10 cells per condition per experiment).

Figure 3. HRS is required for receptor recycling.

A. HeLa cells were treated with siRNA for 120 hours before fixation in 4% PFA/PBS and labelling with antibodies targeting EEA1 and EGFR. B. Pearson's R correlation value between EGFR and EEA1. Single confocal slice images (n=3, all data points plotted, error bars = STD err, >10 images per condition, >150cells total). C. MDA-MB-231 cells were depleted for 120 hours with siRNA before fixation in 4% PFA/PBS and labelling with antibodies targeting EEA1 and EGFR. Single slice images. (n=3, all data points plotted, error bars = STD err, >10 images per condition, >150cells total). D. Pearson's R correlation value between EGFR and EEA1 (n=3, all data points plotted, error bars = STD err, >10 images per condition, >150cells total). E. Cell surface levels of EGFR were measured by flow cytometry, the mean fluorescent intensity was plotted as a percentage of the siNT control for each individual experiment (n=4, error bars = STD err). F. Total EGFR levels in cell lysates normalised to siNT (n=3, error bars = STD err). G. siHRS and control depleted HeLa cells were transfected with photoactivatable GFP-EGFR fusion constructs and mCherry-RAB4, trafficking from the endosome was measured by quantifying the decrease in GFP fluorescence in the endosome normalised to rate of photobleaching (n=9 over two independent experiments). H. MDA-MB-231 cells were treated with the indicated siRNA for 120 hours before being surface labelled with NHS-SS-Biotin on ice and subsequently warmed to generate an internal pool. Than surface biotin was stripped, the cells were warmed for 7.5mins or 15mins to allow for recycling. The cell surface was stripped again to determine the % of recycled receptor compared to total internal pool (n=3, error bars = STD err). Statistical analysis = One-way ANOVA with Dunnett's post-test, except B&H are TTests. Scale bar = 10μm.

Figure 4. HRS is required for activated EGFR recycling.

A. HeLa cells were treated with the indicated siRNA over 120 hours and serum starved for two hours before stimulation with 1ng/ml EGF over the indicated time course and lysis in RIPA buffer (n=3, error bars = STD dev). B. Quantification of degradation normalised to time zero minutes. C-D. Quantification of relative fluorescence intensity of EGFR in EEA1 positive endosomes. Values were normalised to endosome size. C. EGFR endosomal intensity after 30mins treatment with 1ng/ml EGF (n=3, error bars = STD err, approximately >75 cells total). D. EGFR intensity in EEA1 positive endosomes over time course of stimulation with 1ng/ml EGF, values were normalised to timepoint 0 for each condition (n=3, error bars = STD err, approximately >75 cells total). E-G. HeLa cells treated as before, followed by fixation in 4%PFA/PBS and staining with antibodies targeting EEA1 and EGFR. Sum intensity projection images. Statistical analysis = One-way ANOVA with Dunnett's post-test.

Figure 5. HRS is required for MT1-MMP endosomal recycling

A. MDA-MB-231 cells were treated twice with siRNA over 120 hours before fixation and subsequent treatment with Guanidinium hydrochloride. Sum intensity projections. B. Quantification of sum intensity of MT1-MMP in a VPS35 mask (n=50 cells over three independent experiments, Statistical analysis = One-way ANOVA, Dunnett's post test, error bars = STD err). C. MDA-MB-231 cells were treated with siRNA targeting HRS for 120 hours and transfected with photoactivatable (pa)Cherry-MT1-MMP and GFP-EEA1, trafficking from the endosome was measured by quantifying the decrease in paCherry fluorescence in the endosome (n=6 independent experiments, >20cells total, error bars = STD err). Scale bar = 10μm.

Figure 6. Actin binding is required for the efficient sorting of receptors.

HeLa cells were transfected with EGFR and EGFR actin binding mutant YLIP/AAAA (1016-1019) coupled to photoactivatable GFP (paGFP) and mCherry-Rab4. GFP was activated in Rab4 positive endosomes by exposure to 405nm laser light and the rate of recycling was measured by quantifying the decrease in paGFP fluorescence from the endosome. Pre-treatment with 100μM Primaquine to block receptor recycling was used as a negative control. A. Representative activation in Rab4 positive endosomes (taken from Vid.3) (a Gaussian blur has been added). B. Representative traces from an individual experiment (error bars = STD err, >10 cells per experiment per condition, 4 independent experiments). C. MDA-MB-231 with photoactivatable (pa) Cherry fusion MT1-MMP constructs WT or LLY/AAA (571-573) and GFP-EEA1. paCherry constructs were activated in GFP-EEA1 positive endosomes and quantified as above (Graph average traces over three individual experiments, >20 cells total, error bars = STD err).

Figure 7. Actin binding can overcome ubiquitin sorting at the endosome.

A. Schematic of Transferrin receptor (TrfR) chimeras. B. HeLa cells were transfected with indicated constructs and then incubated in 50μg/ml FITC-Trf for 15mins. The cells were washed in PBS and incubated in fresh medium with unlabeled Trf to chase for 1 hour before fixation and staining. C. Pearson's R values between the receptor (myc) and FITC-TrfR were calculated using slidebook software (n=3, 10 images approx. >150cells total, error bars = STD dev). D. HeLa S3 cells were transfected with the TrfR chimeras and treated as before except the recycling was stopped at 0, 15 and 30mins and the retained FITC-Trf was measured by flow cytometry (n≥5, error bars = STD err) E&F. HeLa cells were transfected with indicated fusion constructs for 24hours before treatment with cycloheximide (CHX) to block protein synthesis for the indicated timecourse (n=3, error bars = STD err). All Experiments were performed in the presence of 50μg/ml leupeptin and 100μg/ml cycloheximide except E&F where leupeptin was omitted. Statistical analysis = One-way ANOVA for all comparisons, with Dunnett's post test. Images taken from a single slice. Scale bar = 10μm.

Figure 8. HRS and WASH axis are required for matrix degradation and breast cancer cell invasion.

A. MDA-MB-231 cells were treated with siRNA for 120 hours before being seeded onto 488-Gelatin coated coverslips for 16 hours. B. % of degrading cells (n=3 individual experiments,

approx. >60 cells total, error bars = STD err). Images taken from a single slice. C. MDA-MB-231 cells were treated with siRNA for 96 hours prior to $8x10^4$ cells seeded for an inverted invasion assay on a gel composed of Matrigel/fibronectin followed by culture for 5 days. Images were taken every 10µm and analysed using ImageJ. D. Relative invasion index over 30µm (n=7, (n=3, error bars = STD err). 20ng/ml EGF was used as a chemo-attractant. GM6001 (5µM), DMSO (1:1000) and gels without cells were used as Invasion, vehicle and fibroblast background controls respectively. E Organotypic raft culture. MDA-MB-231 cells were treated with siRNA for 96 hours prior to $7x10^5$ cells seeded on fibroblast remodelled collagen gels and allowed to adhere for 3 days. Gels were then cultured at the liquid-air interface for a further 7 days. Gels were fixed, embedded, H&E stained and sectioned to determine invasion index. F. Quantification of MDA-MB-231 cell invasion relative to siNT control (n=4 independent experiments, error bars = STD err). Statistical analysis = One-way ANOVA for all comparisons with Dunnett's post-test.
Scale bar = 10µm.

Figure 9. Model

A. HRS is required for WASH recruitment and Actin polymerisation on the endosome. B. Actin corrals receptors into an actin meshwork on the endosome that sequesters it into a recycling domain and enabling efficient recycling. Receptor:actin interactions need to be disrupted before ESCRT driven degradation can occur.

Figure S1 HRS is required for the endosomal recruitment of WASH.

A. MDA-MB-231 cells were treated with the indicated siRNA for 120 hours before fixation in 4%PFA/PBS and labelling with antibodies. B. HeLa cells were transfected with Flag-Rab5QL for 24 hours before fixation in 4% PFA and labelling with the indicated antibodies. C. Proximity Ligation Assay (PLA) identifying protein-protein interactions between 10-40nm. Technical control,WASH only antibody. Maximum projection image. D. MDA-MB-231 cells were treated with the indicated siRNA for 120 hours before fixation in 4%PFA/PBS and labelling with antibodies. E. Pearson's R correlation value for WASH and EEA1 (n=3, error bars = STD error, approx. 10 images per condition, >150 cells total). F. HeLa cells were treated with the indicated siRNA for 120hours before fixation in 4%PFA/PBS and labelling with antibodies. G. Pearson's R value for EEA1 and ARPC2 (n=3, error bars = STD err, 30 cells total). H. MDA-MB-231 cells were treated with the indicated siRNA for 120hours before fixation in 4%PFA/PBS and labelling with antibodies. I. Sum intensity value for COMMD1 on EEA1 endosomes (A.U., n=3, error bars = STD error, approx. 10 images per condition, 30 cell total). Statistical analysis = One-way ANOVA for all comparisons with Dunnett's post-test. Scale bar = 10µm. Images show a single slice, except C.

Figure S2 HRS is required for the endosomal recruitment of WASH.

HeLa cells (A-D) and MDA-MB-231 cells (E&F) were treated with siRNA for 120 hours before lysis in RIPA buffer (All blots n=3, One-way ANOVA with Dunnett's post-test). Western blot band intensities were quantified from LI-COR Odyssey scans.

Figure S3. VHS-FYVE domains are sufficient to recruit WASH to the endomembrane.

A&C. Hela cells were treated with siRNA targeting HRS for 120 hours before transfection with GFP or GFP-VHS-FYVE (mHRS 1-226) domain for 24 hours before fixation and antibody labelling for EEA1 and WASH. B. Quantification of Pearson's R correlation value (> 25 cells over 2 independent experiments. error bars= STD err, One-way ANOVA with Dunnett's post-test). Maximum projection images. D. HeLa cells treated as in A were pre-treated with 100µM Primaquine for 30mins before fixation and labelling with the indicated antibodies E. Pearson's R correlation values divided by the siNT control (n=3, approx. 50 cells per condition, 150 cells total, error bars = STD err). Sum intensity images. F. HeLa cells treated with 100µM primaquine for 30mins before fixation and labelling with the indicated antibodies. Sum intensity images. Scale bar = 10µm.

Figure S4. HRS is required for receptor recycling.

A-D. HeLa cells were treated with siRNA for 120 hours before fixation in 4%PFA/PBS and labelling with the indicated antibodies. (Quantification of over 80 cells per condition for a representative experiment, Pearson R values calculated using Image J, 3 independent experiments, error bars = STD err). E. TCA precipitation from the media and lysis in NP40 buffer (representative experiment). F. HeLa cells were treated with siRNA for 120 hours before fixation in 4%PFA/PBS and labelling with the indicated antibodies. Scale bar = 10µm. All images taken from a single slice. Statistical analysis = One-way ANOVA for all comparisons with Dunnett's post-test.

Figure S5. HRS does not affect cell migration over a 2D substrate.

A. MDA-MB-231 cells were treated twice with siRNA over 120 hours before fixation and subsequent treatment with Guanidinium hydrochloride. Images taken from a single slice. B. Western blot of indicated TrfR chimeras transfected into HeLa cells for 24h and immunoprecipitated with myc tag to resolve bands on 8% SDS-PAGE gel. C-F. Cells were sparsely plated on a plastic substrate and imaged for 16hours. Individual cells were tracked using manual tracker Image J plugin, Distance (Accumulated (Total distance covered), Mean Squared Displacement (MSD) (Distance from start position) and directionality (Accumulated distance/MSD) were measured and extracted using chemotaxis ImageJ plugin (n=3 individual experiments, 20 cells per experiment, error bars = STD err).

Video 1.

Hela S3 Flp-in cells stably expressing GFP-mHRS, transfected with mCherry-mWASH on a siWASH treated background.

Video 2.

HeLa cells transfected with indicated siRNA (NT or HRS) for 120 hours were transfected with paGFP-EGFR and mCherry-RAB4. paGFP was activated in mCherry positive endosomes using a pulse of 405nm laser light.

Video 3.

HeLa cells were transfected with paGFP-EGFR/paGFP-EGFR-YLIP/AAAA (actin binding mutant) and mCherry-RAB4. paGFP was activated in RAB4 positive endosomes using a pulse of 405nm laser light.

Video 4.

HeLa cells transfected with either GFP-EGFR or GFP-EGFR-YLIP/AAAA and mRFP-EEA1.

Video 5.

HeLa cells treated with indicated siRNA for 120 hours were transfected with paGFP-EGFR and pCherry4 RAB4. Cells were pretreated with 100mM Primaquine to inhibit recycling before paGFP was activated in mCherry positive endosomes using a pulse of 405nm laser light.

Video 6

MDA-MB-231 cells were transfected with paCherry-MT1-MMP or paCherry-MT1-MMP-LLY/AAA (actin binding mutant) and GFP-EEA1. paCherry was activated in EEA1 positive endosomes using a pulse of 405nm laser light.

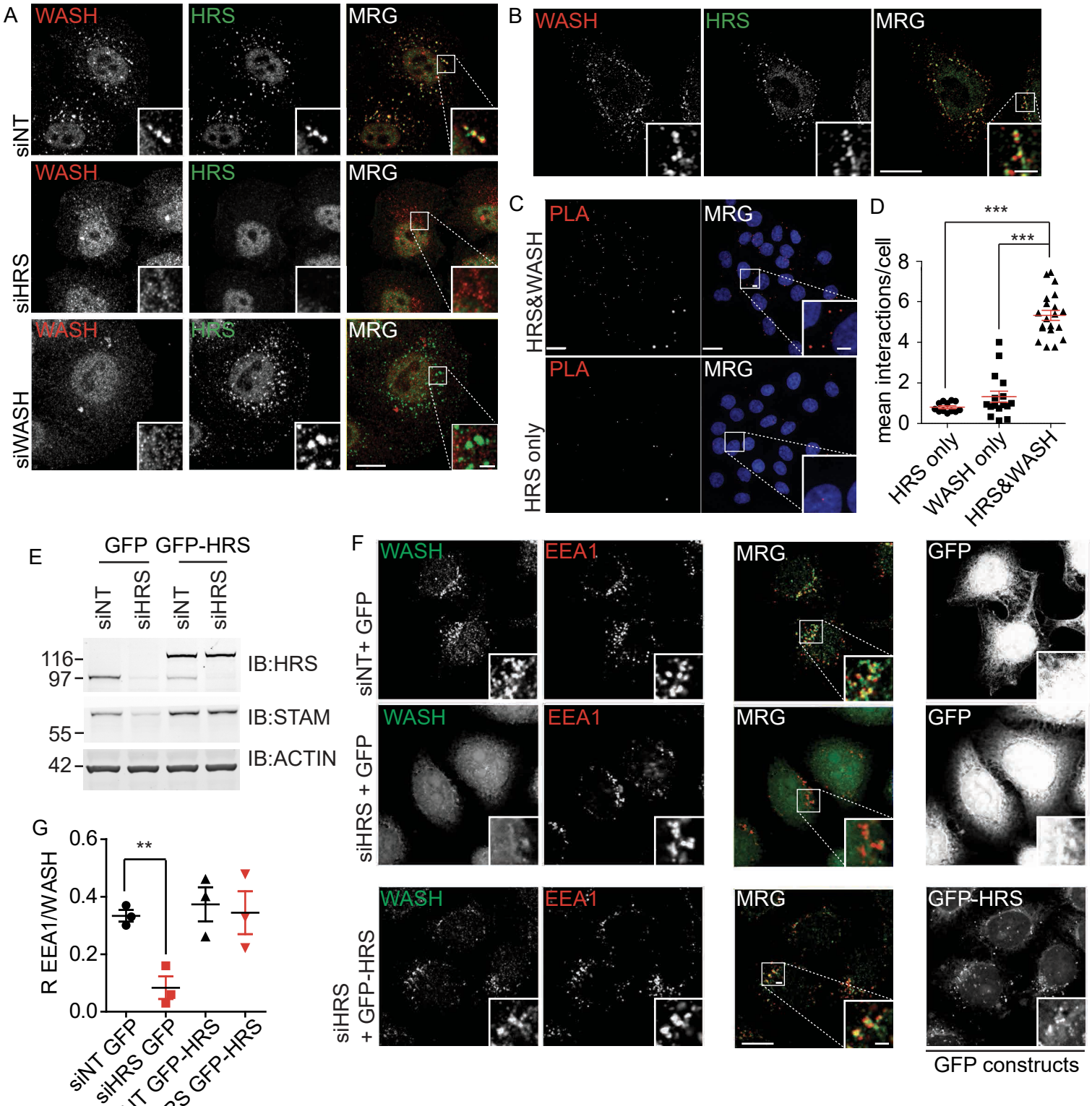


MacDonald et al. Fig 1

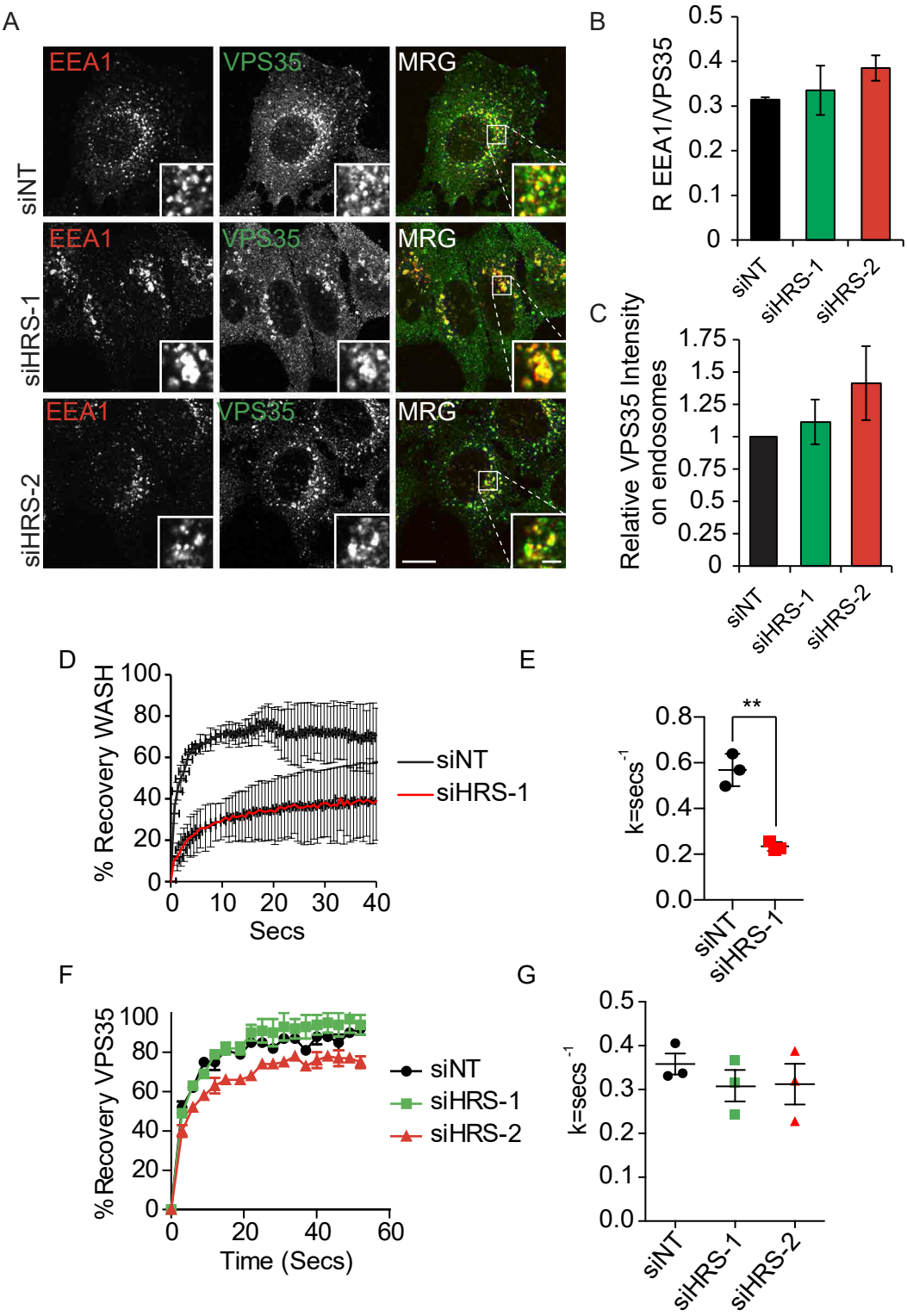


MacDonald et al. Fig2

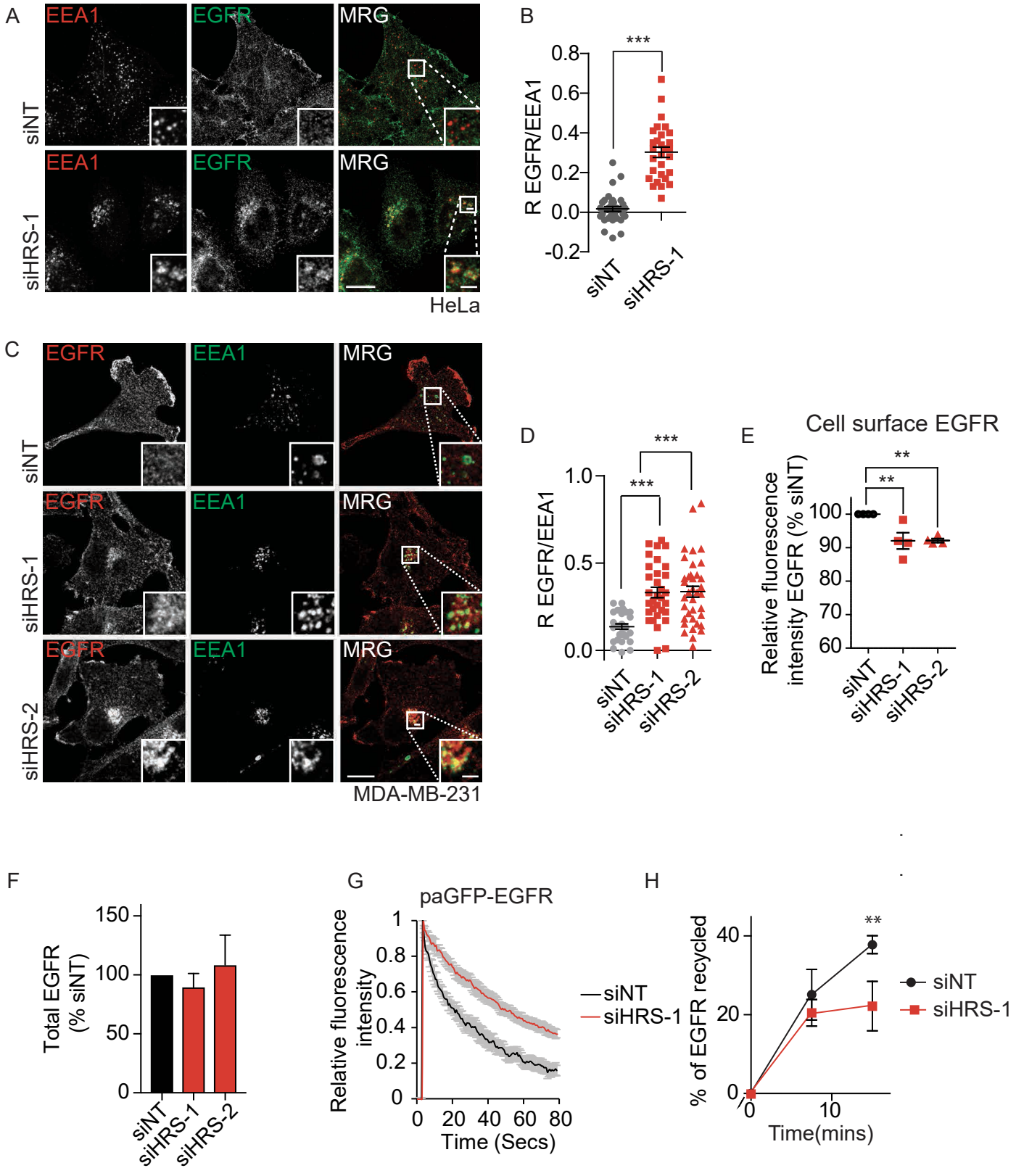


MacDonald et al. Fig 3.

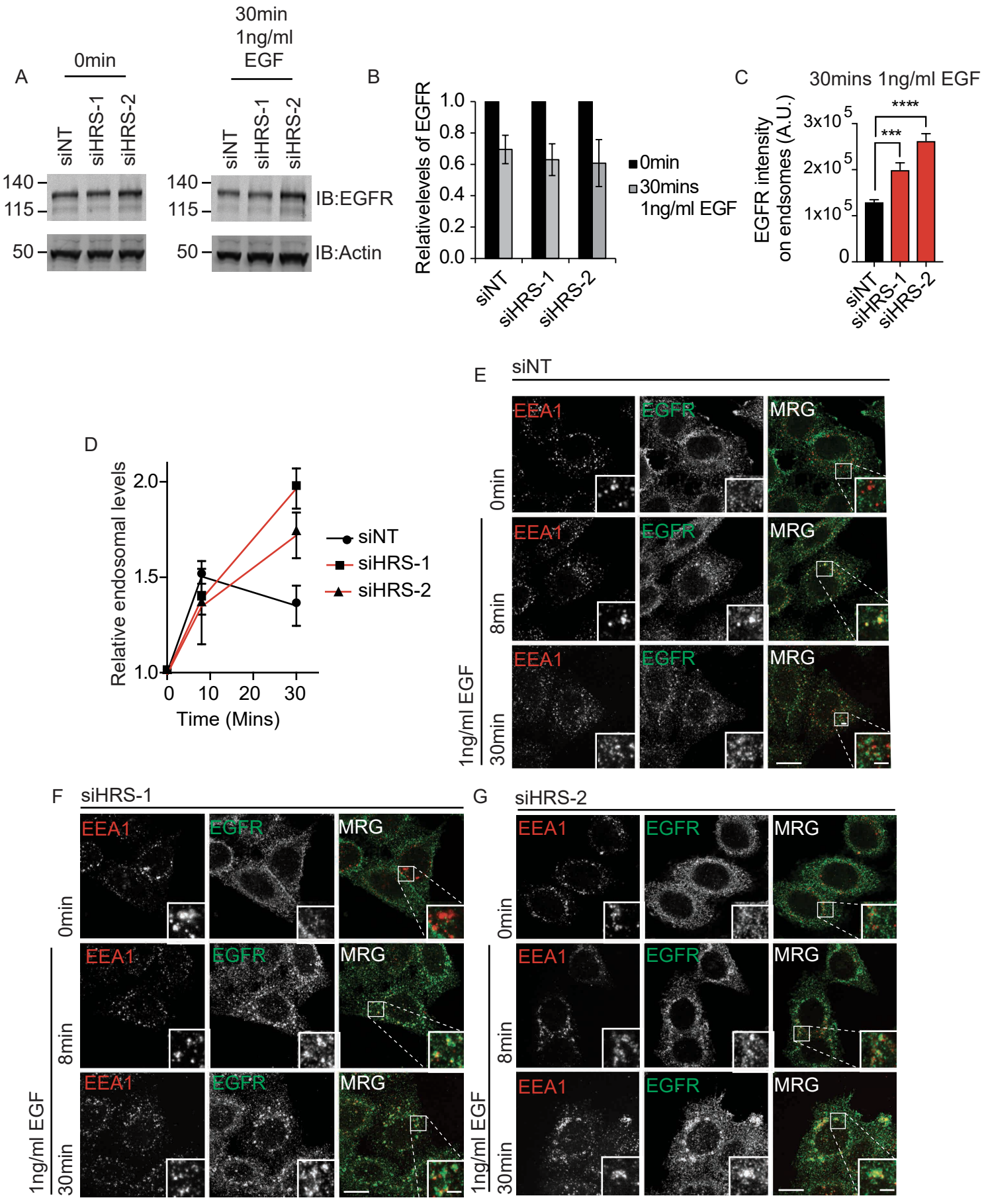
A
0min
30min
1ng/ml
EGF
siNT
siHRS-1
siHRS-2
140
115
50
IB:EGFR
IB:Actin
B
Relativelevels of EGFR
1.0
0.8
0.6
0.4
0.2
0.0
0min
30mins
1ng/ml EGF
C
30mins 1ng/ml EGF
EGFR intensity
on endsomes (A.U.)
3x10 5
2x10 5
1x10 5
0
***
****
D
Relative endosomal levels
2.0
1.5
1.0
0
10
20
30
Time (Mins)
siNT
siHRS-1
siHRS-2
E
siNT
EEA1
EGFR
MRG
0min
8min
30min
1ng/ml EGF
F
siHRS-1
G
siHRS-2

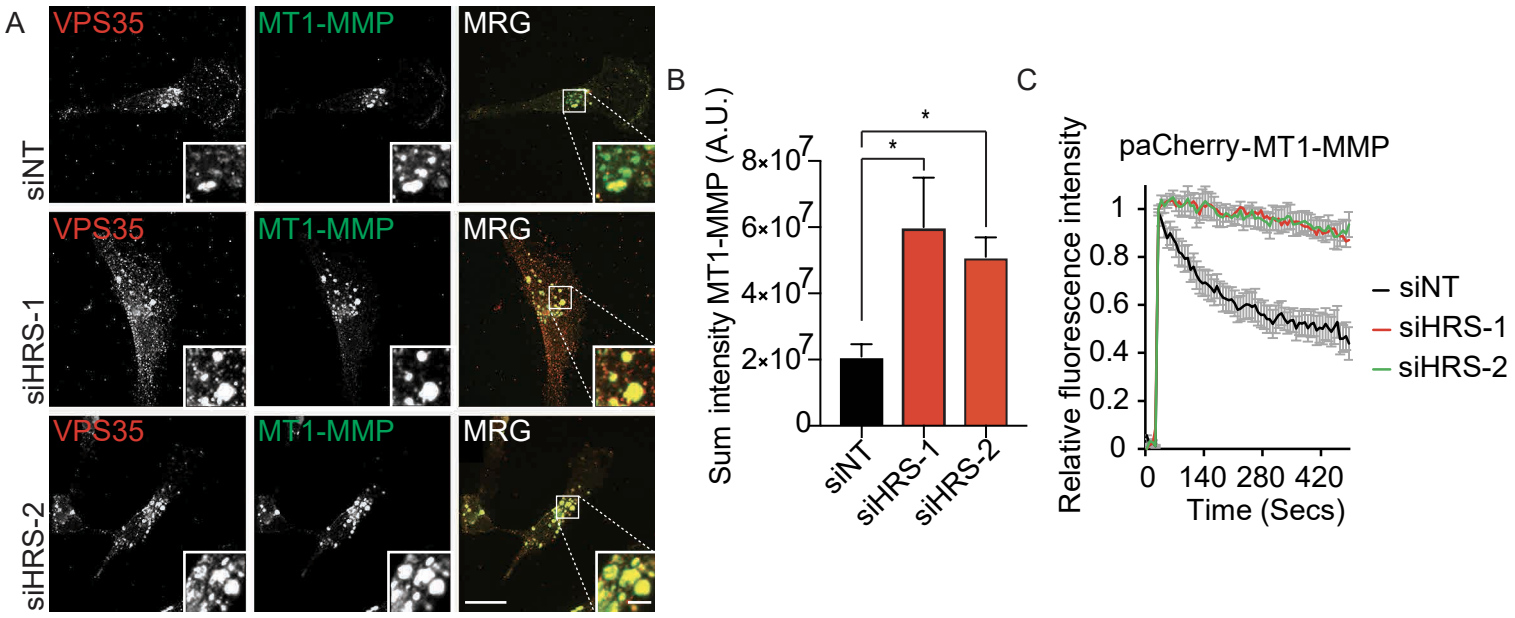


MacDonald et al. Fig 5.

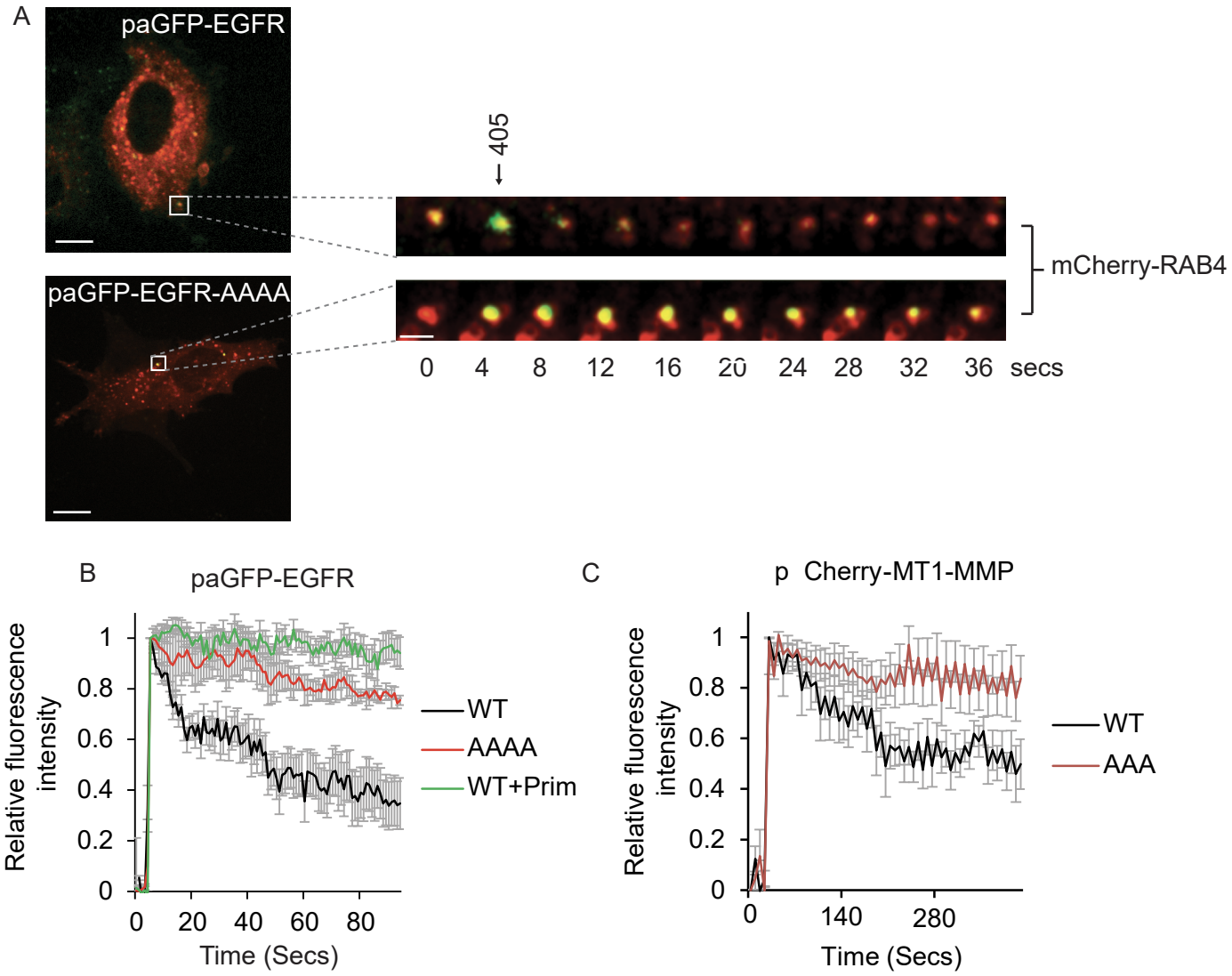


MacDonald et al. Fig 6.

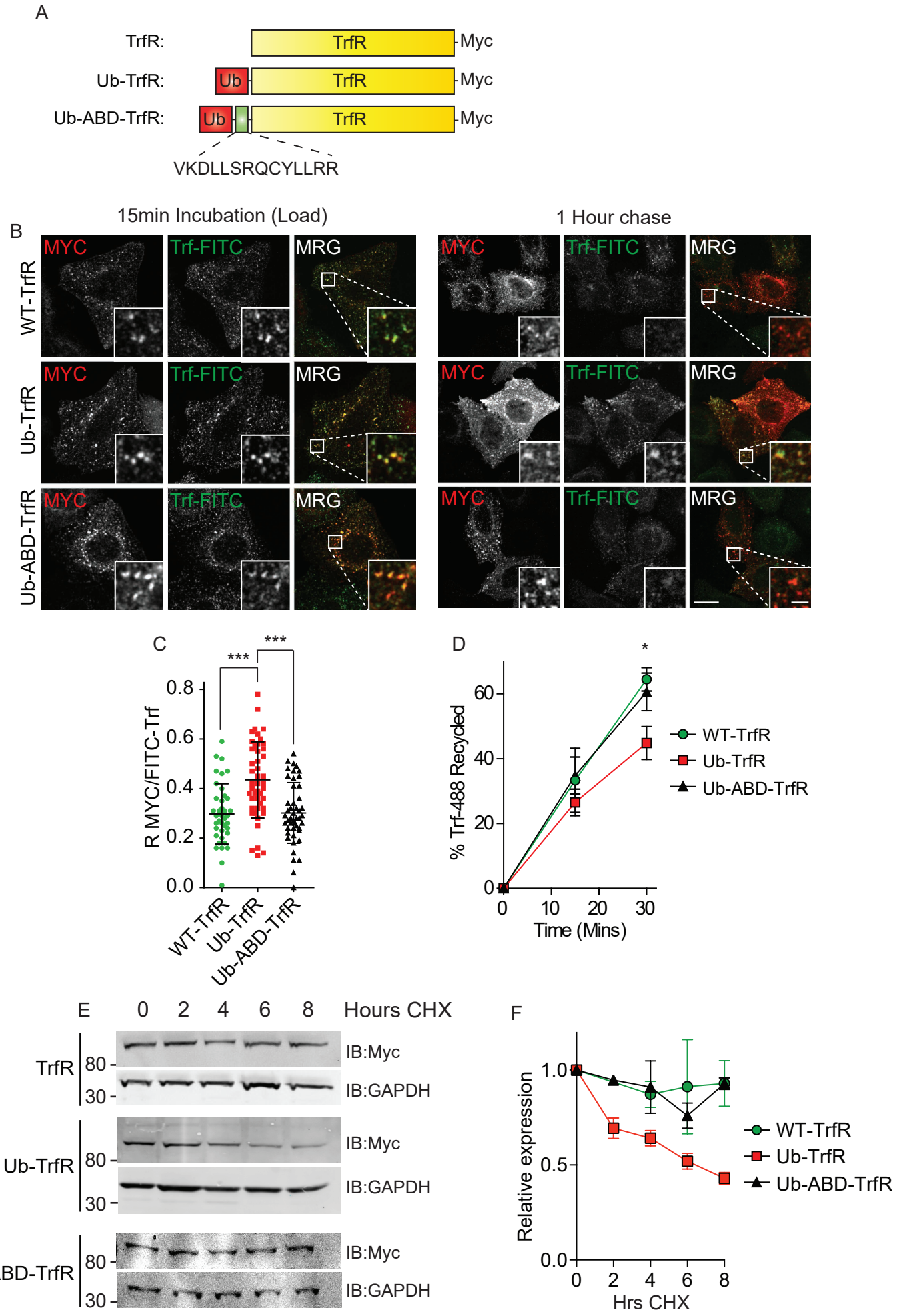


MacDonald et al. Fig 7

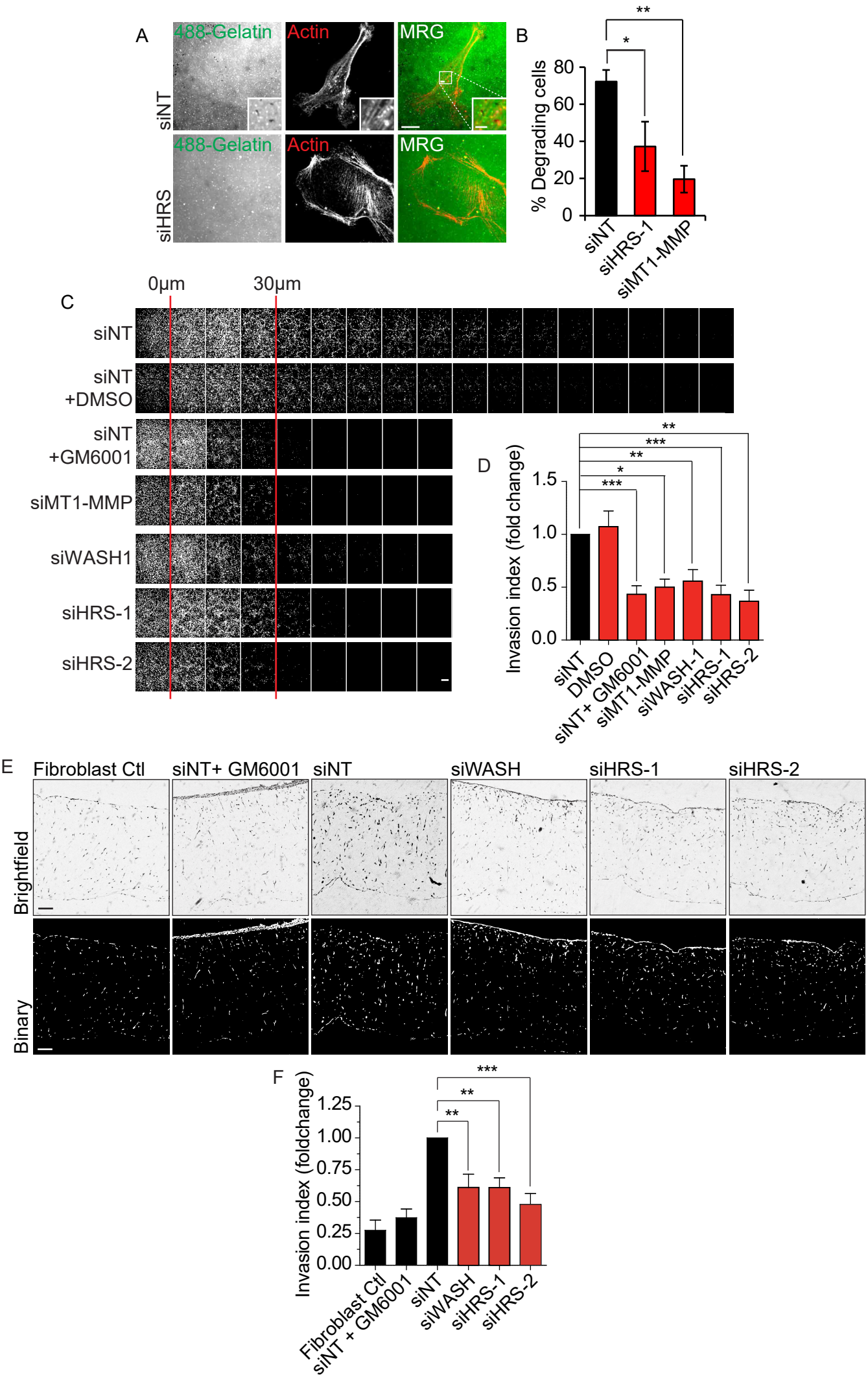


MacDonald et al. Fig 8

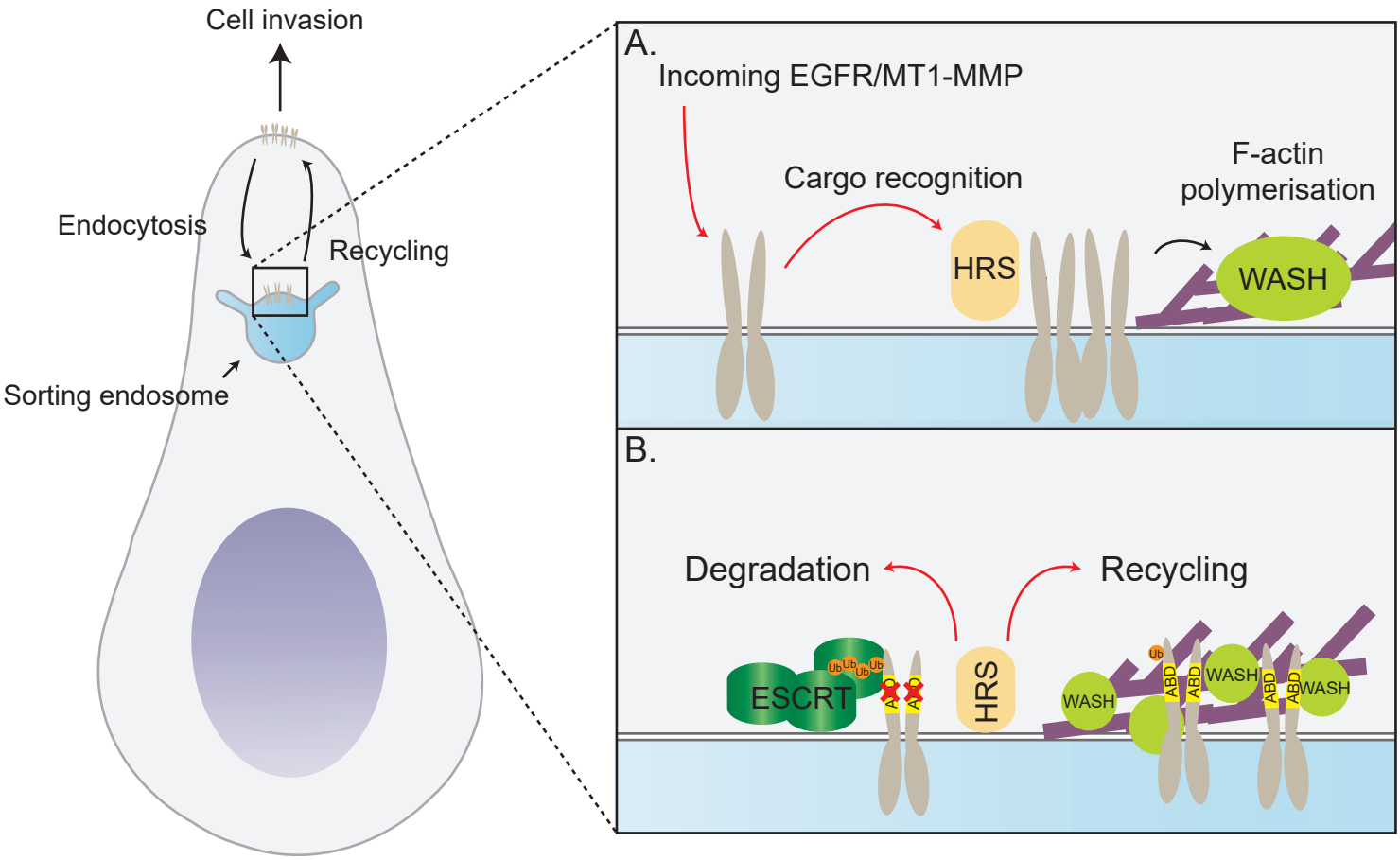


MacDonald et al Fig9

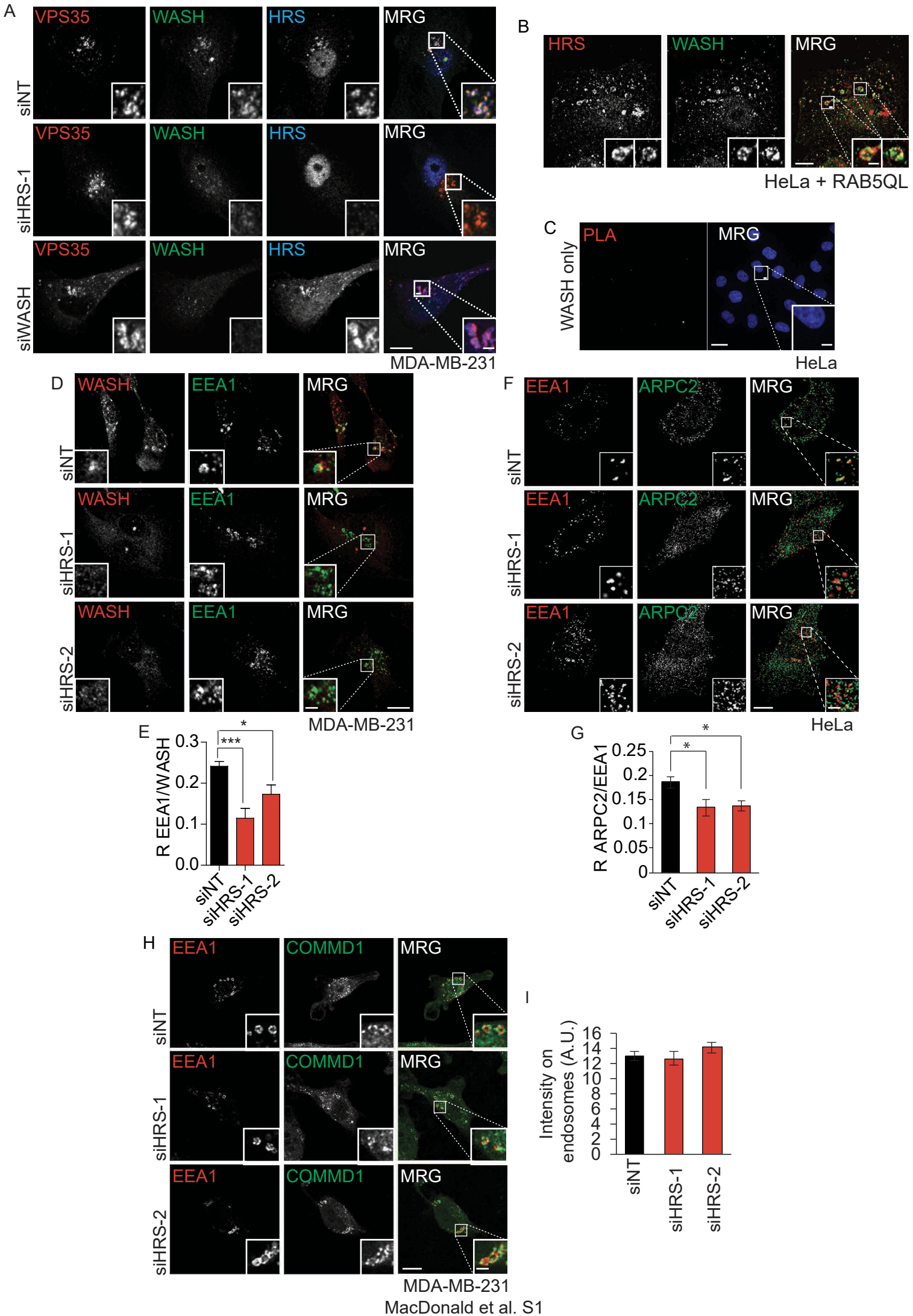


MacDonald et al. S1

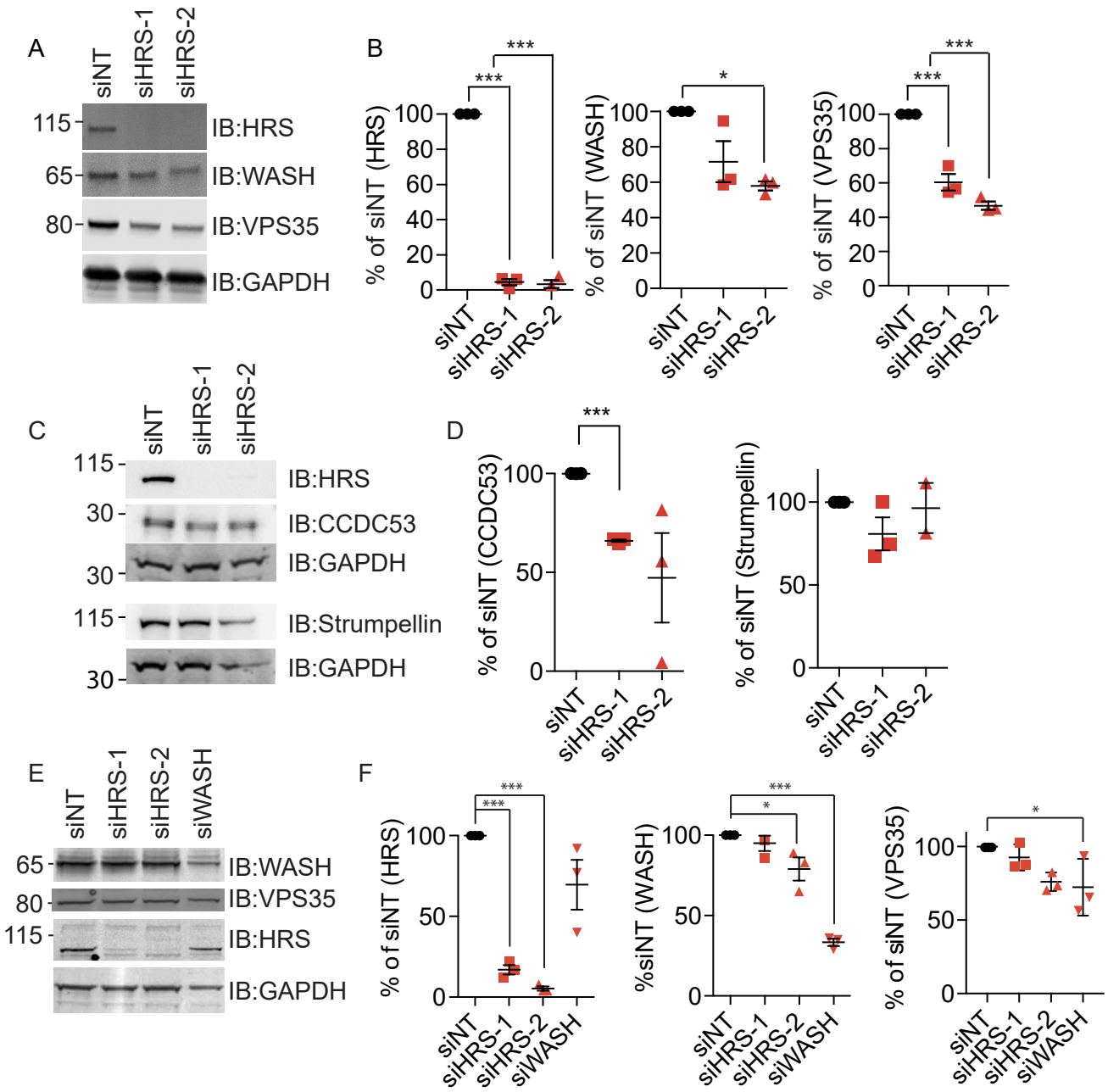
A
siNT
siHRS-1
siHRS-2
115
65
80
IB:HRS
IB:WASH
IB:VPS35
IB:GAPDH
B
% of siNT (HRS)
% of siNT (WASH)
% of siNT (VPS35)
***
*
C
30
IB:CCDC53
IB:Strumpellin
D
% of siNT (CCDC53)
% of siNT (Strumpellin)
E
siWASH
F
%siNT (WASH)

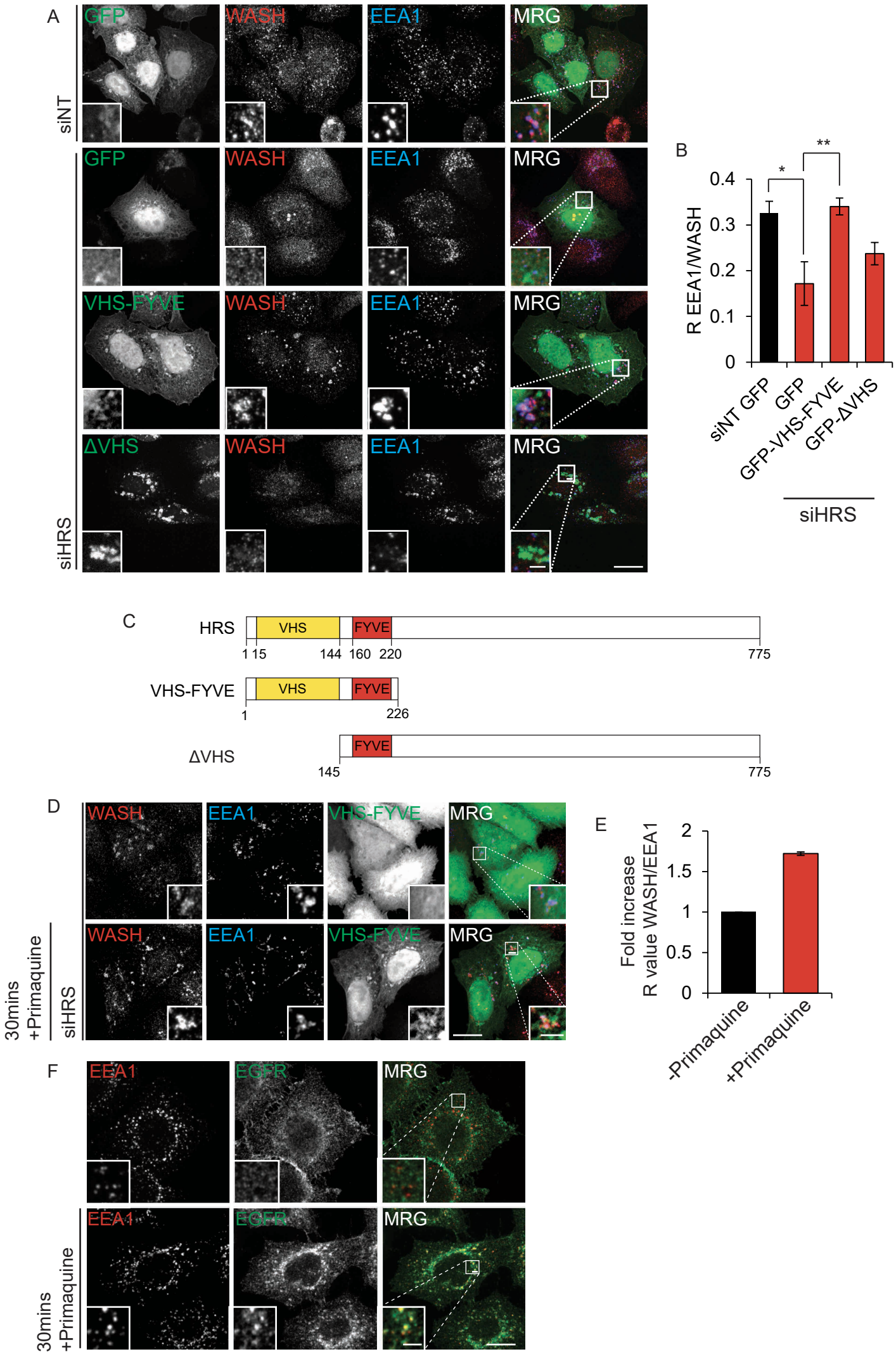
A
GFP
WASH
EEA1
MRG
siNT
GFP
WASH
EEA1
MRG
VHS-FYVE
WASH
EEA1
MRG
ΔVHS
WASH
EEA1
MRG
siHRS
B
R EEA1/WASH
0.4
0.3
0.2
0.1
0
*
**
siNT GFP
GFP
GFP-VHS-FYVE
GFP-ΔVHS
siHRS
C
HRS
VHS
FYVE
1 15
144
160
220
775
VHS-FYVE
VHS
FYVE
1
226
ΔVHS
FYVE
145
775
D
WASH
EEA1
VHS-FYVE
MRG
30mins +Primaquine
siHRS
E
Fold increase R value WASH/EEA1
2
1.5
1
0.5
0
-Primaquine
+Primaquine
F
EEA1
EGFR
MRG
30mins +Primaquine

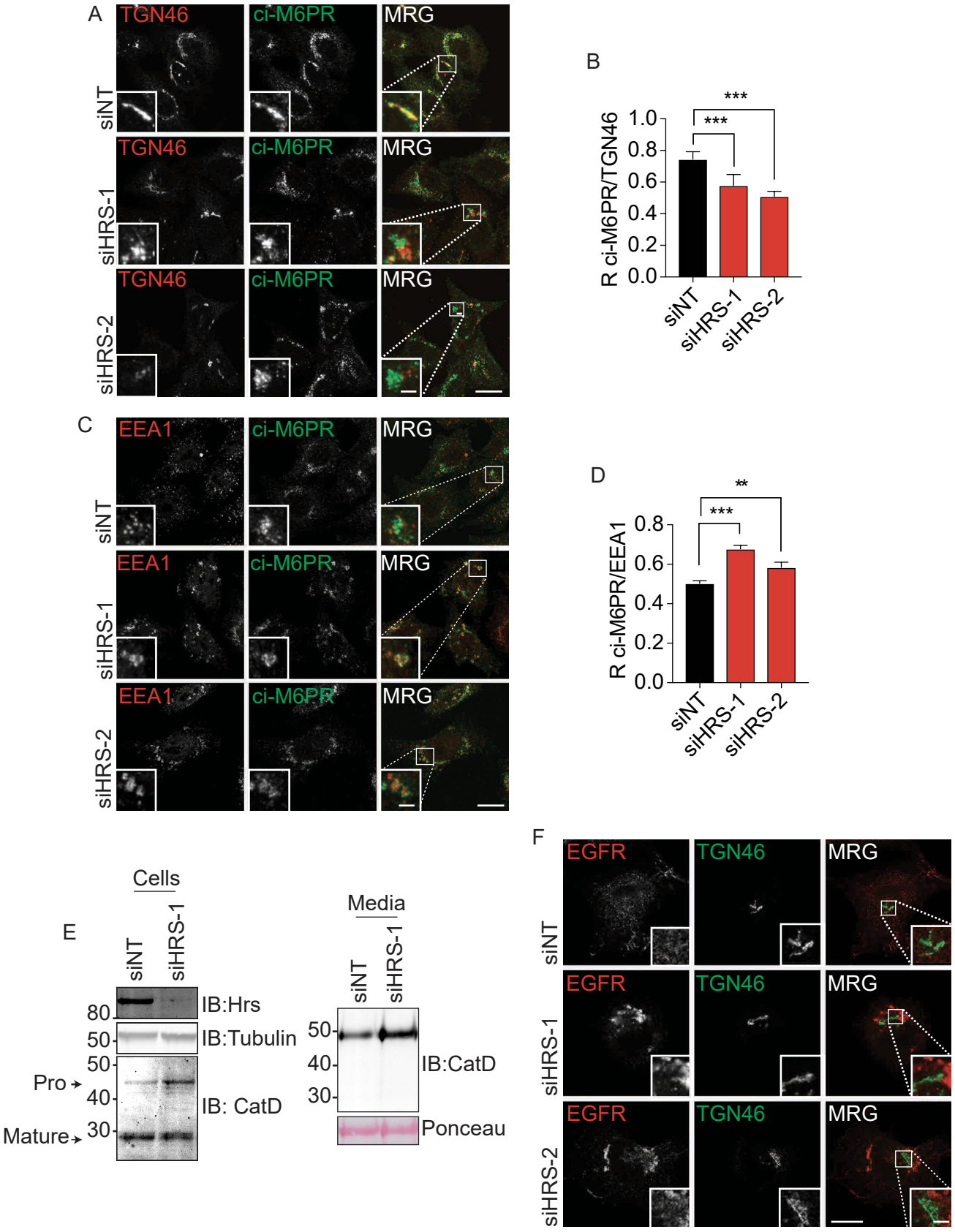
A
TGN46
ci-M6PR
MRG
siNT
siHRS-1
siHRS-2
B
R ci-M6PR/TGN46
1.0
0.8
0.6
0.4
0.2
0.0
***
***
siNT
siHRS-1
siHRS-2
C
EEA1
ci-M6PR
MRG
siNT
siHRS-1
siHRS-2
D
R ci-M6PR/EEA1
0.8
0.6
0.4
0.2
0.0
**
***
siNT
siHRS-1
siHRS-2
E
Cells
Media
siNT
siHRS-1
80
50
IB:Hrs
IB:Tubulin
50
Pro
40
Mature
30
IB: CatD
50
40
30
IB:CatD
Ponceau
F
EGFR
TGN46
MRG
siNT
siHRS-1
siHRS-2

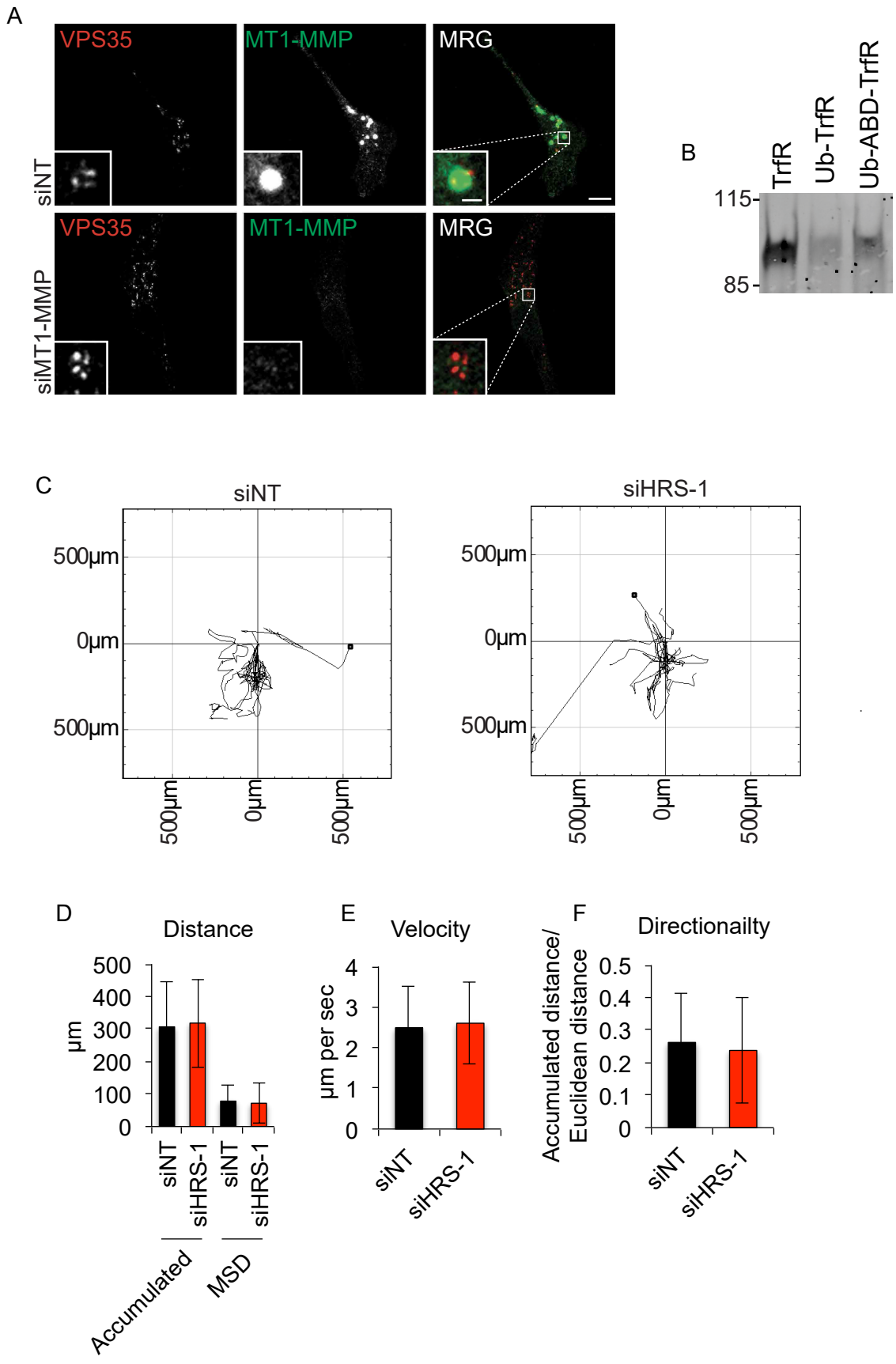
A
VPS35
MT1-MMP
MRG
siNT
siMT1-MMP
B
TrfR
Ub-TrfR
Ub-ABD-TrfR
115
85
C
siNT
siHRS-1
500µm
0µm
D
Distance
µm
Accumulated
MSD
E
Velocity
µm per sec
F
Directionailty
Accumulated distance/
Euclidean distance
siNT
siHRS-1